

1
2
3
4
5
6
7
8
9
10
11
12
13
14
15
16
17
18
19
20
21
22
23
24
25
26
27
28
29
30
31
32
33

Coordination of rooting, xylem, and stomatal strategies explains the response of conifer forest stands to multi-year drought in the Southern Sierra Nevada of California

Junyan Ding^{1,2}, Polly Buotte³, Roger Bales⁴, Bradley Christoffersen⁵, Rosie A. Fisher^{6,7}, Michael Goulden⁸, Ryan Knox¹, Lara Kueppers^{1,3}, Jacquelyn Shuman⁶, Chonggang Xu⁹, Charles D. Koven¹

1. Climate and Ecosystem Sciences Division, Lawrence Berkeley National Lab, Berkeley, USA
2. Pacific Northwest National Lab, Richland, WA, USA
3. Energy and Resources Group, University of California, Berkeley, USA
4. Sierra Nevada Research Institute, University of California, Merced, USA
5. Department of Biology, University of Texas, Rio Grande Valley, USA
6. Climate and Global Dynamics Division, National Center for Atmospheric Research, Bold, USA
7. Laboratoire Évolution & Diversité Biologique, CNRS:UMR 5174, Université Paul Sabatier, Toulouse, France
8. Dept. of Earth System Science, University of California, Irvine, USA
9. Earth and Environmental Sciences Division, Los Alamos National Laboratory, Santa Fe, New Mexico, USA

Corresponding author: Junyan Ding (junyan.ding@pnnl.gov)

Key Points:

- We perform a sensitivity analysis using the model FATES-Hydro to explore the ~~eo-~~ordination of leaf, xylem, and root hydraulic traits of pine in the Southern Sierra Nevada.
- We find that rooting depth is the major control on water and carbon fluxes, and that deep-rooted pines with risky stomata have the highest GPP but also the highest drought mortality risk.
- Resolving both ~~the~~ plant water sourcing strategies and subsurface processes ~~are~~is critical to ~~represent~~representing drought impacts on conifer forests.

34

Abstract

35 Extreme droughts are a major determinant of ecosystem disturbance, which ~~impact~~impacts
36 plant communities and ~~feed~~feeds back ~~to~~into climate change through changes in plant
37 functioning. However, the complex relationships between above- and ~~belowground~~below-
38 ground plant hydraulic traits, and their role in governing plant responses to drought, are not
39 fully understood. In this study, we use a plant hydraulic model, FATES-Hydro, to investigate
40 ecosystem responses to the 2012–2015 California drought, in comparison with observations,
41 ~~for~~at a site in the southern Sierra Nevada that experienced widespread tree mortality during
42 this drought.

43 We conduct a sensitivity analysis to explore how different plant water sourcing and hydraulic
44 strategies lead to differential responses during normal and drought conditions.

45 The analysis shows that:

- 46 1. ~~deep~~Deep roots that sustain productivity through the dry season are needed for the model
47 to capture observed seasonal cycles of ET and GPP in normal years, and ~~that~~-deep-rooted
48 strategies are nonetheless subject to large reductions in ET and GPP when the deep soil
49 reservoir is depleted during extreme droughts, in agreement with observations.
- 50 2. ~~risky~~Risky stomatal strategies lead to greater productivity during normal years as compared
51 to safer stomatal control, but they also lead to a high risk of xylem embolism during the
52 2012–2015 drought.
- 53 3. ~~for~~For a given stand density, ~~the~~-stomatal and xylem traits have a stronger impact on plant
54 water status than on ecosystem-level fluxes.

55 Our study ~~reveals~~highlights the ~~importance~~significance of resolving plant water sourcing
56 strategies ~~in order~~-to represent drought impacts on plants, and consequent feedbacks, in
57 models.

58

59

60 1. Introduction

61 Understanding plant water use strategies and the resulting ecohydrologic processes in
62 forests is critical for predicting surface water and energy exchange, carbon dynamics, and
63 vegetation dynamics of water-constrained ecosystems in a changing climate. Mediterranean-type
64 climates, as in California, are characterized by dry and hot summers and cool, wet winters,
65 resulting in asynchronous supplies of energy and water. In addition to these climatic stresses,
66 plants in California are further subject to high inter-annual variability in precipitation, and
67 periodic severe drought events, such as the recent 2012—2015 drought, which led to
68 widespread tree mortality (Fettig et al. 2019). Together, these two climatic constraints
69 ~~bring present~~ a unique challenge to the success of forests in California, which ~~are is~~ likely to be
70 exacerbated ~~in by~~ a warming climate.

71 On evolutionary timescales, natural selection has led to a wide array of strategies and
72 functional traits that allow plants to both grow and survive under a range of
73 ~~environment~~environmental conditions (Grime 1977, 1979; Coley et al. 1985; Westoby et al.
74 2002; Craine 2002; Reich et al. 2003). Given the centrality of water sourcing ~~ont~~ plant
75 physiology, plant hydraulic traits play an important role in water-constrained ecosystems. Once
76 absorbed by fine roots, water flows through the vascular system via coarse roots, stems, and
77 branches, to leaves, where it evaporates through stomata. The rate of water flow through stems,
78 and thus the supply to leaves, is determined by the hydraulic conductivity along this pathway. If
79 the water potential of xylem tissue becomes too low, cavitation can occur and cause a loss of
80 conductivity. Because this cavitation can damage the xylem network, trees have developed
81 different strategies to mitigate this effect, all of which come at some cost. These strategies
82 include 1) early stomatal closure or leaf deciduousness to reduce the flow of water, at the cost of
83 reduced carbon intake; 2) building cavitation-resistant xylem, at the cost of increased hydraulic
84 resistance; and 3) growing deep roots to access more moisture, at the cost of higher carbon
85 investment. In this study, we focus on the potential hydraulic strategies that trees in Californian
86 ecosystems use, with a particular emphasis on how the ~~co-ordination~~coordination of hydraulic
87 functional traits at the leaf, stem, and root levels is critical to carbon assimilation, transpiration,
88 and consequently, the productivity and ~~the~~ response of trees to drought (Matheny, Mirfenderesgi,
89 and Bohrer 2017; Matheny et al. 2017; Mursinna et al. 2018a).

90 The traits that regulate stomatal conductivity are the most important hydraulic traits of
91 leaves and the primary ones through which photosynthesis and transpiration are coupled.
92 Stomatal behavior falls along a gradient between two extremes: stomata may close early during
93 water stress to avoid the risk of hydraulic failure, or remain open to maximize carbon uptake
94 while exposing xylem to a higher risk of embolism (Martínez-Vilalta, Sala, and Piñol, 2004;
95 McDowell et al., 2008; Skelton, West, & Dawson, 2015; Matheny et al., 2017). The sensitivity
96 of stomata to water stress determines where the stomata operate along the safety-~~risky~~risk
97 gradient, and thus the degree ~~that~~ to which carbon intake is traded for preventing the cavitation
98 of xylem. Where the best stomatal strategy sits along the safety-~~risky~~risk gradient would depend
99 on the physical environment.

100 ~~The maximum~~Maximum hydraulic conductivity and ~~the~~ vulnerability to cavitation are the
101 two key xylem hydraulic traits. Differences in the anatomy and morphology of the conductive
102 xylem cell structure and anatomy (Hacke et al. 2017) lead to differences in maximum
103 conductivity and the water potential at which cavitation starts to occur (Pockman & Sperry,
104 2000; Sperry 2003). Within the conifers, there are at least three mechanisms that lead to a
105 tradeoff between xylem safety and efficiency. ~~First~~The first is the morphology of the xylem
106 conduit. It is widely acknowledged that narrow (or short) tracheid are safer than wider (or
107 longer) tracheid but have lower conductance per sap area (Choat and Pittermann 2009). Second
108 are the intervessel pit membranes. Thicker and less porous membranes prevent the spread of air
109 but increase the hydraulic resistance of xylem (e.g., Li et al., 2016; Pratt & Jacobsen, 2017). The
110 third mechanism comes from the division of limited space (Pratt and Jacobsen 2017). With the
111 same cross-sectional area of conduits, vessels with a thicker cell wall provide stronger
112 mechanical support, so that the conduits are less likely to collapse when xylem water potential
113 becomes more negative; however, this reduces the area that can be used for conduits
114 transporting water. While these physiological constraints require that the tradeoff ~~does exist~~exists
115 to some extent, in many studies, this tradeoff appears to be weak, and there are certainly species
116 that have both safe and efficient xylem. Further, there are many other plant traits that can affect
117 ~~the safety~~, such as wood density (Pratt and Jacobsen 2017), pit anatomy (Sperry & Hacke 2004,
118 Lens et al. 2011), and biochemistry (Gortan et al. 2011). These traits can have large
119 ~~variation~~variations among different plant types. The tradeoff will be weakened when grouping
120 plants at a coarse scale, e.g., by biomass, families, and/or across a range of geological and

121 climatic ~~region~~regions. But when focusing on certain species in a particular region, the tradeoff
122 becomes stronger, as demonstrated by many local studies (e.g., Barnard et al. 2011, Corcuera et
123 al. 2011, Baker et al. 2019). For example, Kilgore et al. (2021) ~~shows~~show that there is a clear
124 safety-efficiency tradeoff across pine trees in a specific location in the western US. Thus, while
125 we acknowledge that there are many exceptions to the xylem safety-efficiency tradeoff, it is a
126 useful framework for examining plant strategies for dealing with drought.

127 The traits that govern the hydraulic function of plant root systems are also critically
128 important, but ~~they are~~ the least understood, studied, and quantified. These traits include the
129 rooting depth, the root-to-shoot ratio, the vertical and lateral distribution of roots, and the fine
130 root density and diameter, all of which are related to water uptake (Canadell et al., 2007; Allen,
131 2009; Reichstein et al., 2014; Wullschlegel et al., 2014). In general, species with deeper roots
132 can access water at greater depths, ~~that, which~~ is unavailable to more shallowly rooted species
133 (Jackson et al., 1996; Canadell et al., 1996). The vertical root distribution can affect the water
134 uptake and thus the evapotranspiration (ET) pattern during the dry-down period (Teuling,
135 Uijlenhoet, and Troch 2006). This in turn affects the seasonal distribution of water over the soil
136 depth, and thereby the resilience of plants to seasonal droughts (Yu, Zhuang, and Nakayamma
137 2007). The vertical root distribution is also a means of belowground niche differentiation (Ivanov
138 et al. 2012; Kulmatiski and Beard 2013), whereas the extent of the lateral root distribution
139 dictates the competition for water (Agee et al. 2021). Whether a plant can benefit from having
140 deep roots is related to the ~~plant's~~plant's leaf and xylem hydraulic traits (e.g., Johnson et al.
141 2018, Mackay et al. 2020), thus requiring coordination of rooting and hydraulic traits.

142 Given the strength of the Mediterranean-type climate of California, the coordination of
143 rooting and hydraulic strategies will play a critical role ~~for~~in forest dynamics. However, the
144 interplay of rooting and hydraulic strategies and their impact on ecosystem processes
145 ~~haven't~~haven't been well understood. In this study, we address this question at the Soaproot site
146 (CZ2) of the southern Sierra Nevada of California as the study area. The CZ2 site was strongly
147 affected by the 2012–2015 drought, with extremely high tree mortality rates (~~~~~90% of the pine
148 died) (Fettig et al. 2019). While the 2012–2015 drought was widespread across California, the
149 highest rates of tree mortality occurred in the southern Sierra Nevada, centered around an
150 elevation similar to this site (1160 m to 2015 m, Asner et al. 2016, Goulden and Bales 2019).

151 This mid-elevation region is also characterized by the highest forest productivity along an
152 elevation gradient from foothill woodlands to subalpine forest (Kelly and Goulden 2016). This
153 leads us to ask whether strategies associated with high productivity have exposed trees to a high
154 mortality risk under prolonged drought.

155 Specifically, here we use the Functionally Assembled Terrestrial Ecosystem Simulator, in
156 a configuration that includes plant hydraulics (FATES-Hydro), to explore the tradeoffs
157 associated with differing hydraulic strategies, and in particular, their implications for plant
158 productivity and the risk of drought-induced mortality. We conduct a sensitivity analysis, using
159 FATES-Hydro in comparison with observations from the CZ2 eddy covariance site, to
160 investigate how stomatal, xylem, and rooting strategies affect the ecosystem and physiologic
161 processes of the forest, and whether that may explain the high rates of both productivity and
162 drought-associated mortality of conifers at CZ2. We note that this is not ~~an~~ exhaustive model
163 parameter sensitivity study. ~~The~~The main purpose is to use a sensitivity analysis to explore
164 scientific questions around hydraulic trait tradeoffs.

165 2. Methods

166 2.1 Study site

167 The Soaproot site is a 543-ha headwater catchment at 1100m elevation (37°2.4' N,
168 119°15.42' W), which is at the lower boundary of the rain–snow transition line with warm, dry
169 summers and cool, wet winters (Geen et al. 2018). The mean annual temperature is about 13.8°C
170 (Goulden et al., 2012). Under normal conditions, the annual precipitation is about 1300 mm, but
171 during a dry year, the precipitation can drop to 300-600mm. (Bales et al. 2018). The site is a
172 ponderosa pine (*Pinus ponderosa*) dominated conifer ecosystem exhibiting high productivity
173 (Kelly and Goulden (2016) reported 2.1 tC/ha/year average annual gross stem wood production
174 averaged). Other species include California black oak (*Quercus kelloggii* Newberry), and incense
175 cedar (*Calocedrus decurrens*).

176 Soils at the Soaproot site are mainly of the Holland (fine-loamy, mesic Ultic Haploxeralfs)
177 and Chaix (coarse-loamy, mesic Typic Dystroxerepts) series, which are representative of soils
178 across a similar elevation band of the western Sierra Nevada (Mooney and Zavaleta 2003). Soils
179 of the Holland series have sandy loam surface texture and underlying Bt horizons with sandy

180 clay loam textures, while soils of the Chaix series have sandy loam textures throughout the
181 profile. The regolith depth is estimated to be 15m (Holbrook et al., 2014). The total porosity over
182 the whole regolith depth of the site is estimated to be 1620 mm and the total available storage
183 porosity (plant accessible water storage capacity), which is the difference in volumetric water
184 content between field capacity and permanent wilting point ($\sim -6\text{Mpa}$) to be 1400 mm (Klos et
185 al. 2017). The available water storage capacity is approximately $0.20\text{ cm}^3\text{ cm}^{-3}$ in the upper
186 regolith (0–5 m depth) which decreases to $0.05\text{ cm}^3\text{ cm}^{-3}$ or less in the lower regolith (below 5
187 m depth) (Holbrook et al., 2014).

188 An eddy-covariance flux tower was installed at this site in September 2010. The elevation
189 of the tower is 1160 m above sea level. Instruments on the flux tower track changes in carbon
190 dioxide, water vapor, air temperature, relative humidity, and other atmospheric properties. We
191 compare the simulated gross primary productivity (GPP) and latent heat flux with the flux tower
192 measurements over the period from 2011 to 2015 (Goulden and Bales 2019). We computed the
193 Root Mean Square Error (RMSE) of the hourly mean diurnal cycle of each month. This allows
194 us to examine the capacity of FATES-Hydro to predict the carbon and water fluxes. The
195 transpiration at the site contributed to the majority of the ET as indicated by the measurements
196 from an adjacent catchment, as well as the fact that the site is fully vegetated with an annual LAI
197 around 3 to 4.

198

199 2.2 FATES-Hydro model and parameterization

200 2.2.1 The FATES-Hydro model

201 FATES is a cohort-based, size- and age-structured dynamic vegetation model, where long-
202 term plant growth and mortality rates and plant competition emerge as a consequence of
203 physiological processes. In the model, multiple cohorts grow on the same land unit, share the soil
204 water, and interact with each other through light competition. FATES is coupled within both the
205 CLM5 (Lawrence et al., 2019) and the ELM (Golaz et al., 2020) land surface models (LSMs). In
206 this study, FATES is coupled with the CLM5. FATES-Hydro is a recent development of the
207 FATES model (Fisher et al., 2015; Koven et al., 2020), in which a plant hydro-dynamic module,
208 originally developed by Christoffersen et al. (2016), is coupled to the existing photosynthesis and

209 soil hydraulic modules. FATES-Hydro is described in more detail by Xu et al., (in review,
 210 <https://doi.org/10.5194/egusphere-2023-278><https://doi.org/10.5194/egusphere-2023-278>) and its
 211 supplementary material.

212 Conceptually, plant hydraulic models can be broadly grouped into two types. The first
 213 group represents the plant hydraulic system as analogous to an electrical circuit (e.g. Mackay et
 214 al. 2011, Huang et al. 2017, Eller et al. 2018, Kennedy et al. 2019). The total resistance of the
 215 plant is calculated from the resistance of each compartment using Ohm’s law. There is no storage
 216 of water in the plants and the transpiration from plants at any given time step is considered to
 217 come directly from soil storage. The second group represents plant hydraulics by a series of
 218 connected porous media, corresponding to each plant compartment (e.g. Bohrer et al. 2005,
 219 Janott et al. 2011, Xu et al., 2016, Christoffersen et al., 2016). The porous media model takes
 220 into account the water storage in the plant. The flow between two adjacent compartments is
 221 driven by the difference in the water potential, mediated by the hydraulic conductivity. FATES-
 222 Hydro falls in the second group. The various models in the second group differ in the exact
 223 formulas used to describe the pressure-volume and pressure-conductivity relations, as well as
 224 different numbers and arrangement of nodes within the soil-plant-atmosphere system.

225 In FATES-Hydro, for each plant cohort, the hydraulic module tracks water flow along a
 226 soil–plant–atmosphere continuum of a representative individual tree based on hydraulic laws,
 227 and updates the water content and potential of leaves, stem, and roots with a 30 minute model
 228 time step. Water flow from each soil layer within the root zone into the plant root system is
 229 calculated as a function of the hydraulic conductivity as determined by root biomass and root
 230 traits such as specific root length, and the difference in water potential between the absorbing
 231 roots and the rhizosphere. The vertical root distribution is based on Zeng's (2001) two parameter
 232 power law function, which takes into account the regolith depth:

$$Y_i = \frac{0.5(e^{-r_a z_{li}} + e^{-r_b z_{li}}) - 0.5(e^{-r_a z_{ui}} + e^{-r_b z_{ui}})}{1 - 0.5(e^{-r_a z} + e^{-r_b z})} \quad Y_i = \frac{0.5(e^{-r_a z_{li}} + e^{-r_b z_{li}}) - 0.5(e^{-r_a z_{ui}} + e^{-r_b z_{ui}})}{1 - 0.5(e^{-r_a z} + e^{-r_b z})}$$

234 (Eq 1)

235 where Y_i is the fraction of fine or coarse roots in the i th soil layer, r_a and r_b are the two
 236 parameters that determine the vertical root distribution, Z_{li} is the depth of the lower boundary of

237 the i th soil layer, and Z_{ui} is the depth of the upper boundary of the i th soil layer, and Z is the total
 238 regolith depth. The vertical root distribution affects water uptake by the hydrodynamic model by
 239 distributing the total amount of root, and thus root resistance, through the soils.

240 The total transpiration of a tree is the product of total leaf area (LA) and the transpiration
 241 rate per unit leaf area (J). In this version of FATES-Hydro, we adopt the model developed by
 242 Vesala et al. (2017) to take into account the effect of leaf water potential on the within-leaf
 243 relative humidity and transpiration rate:

$$E = LA \cdot J \quad (\text{Eq 2a})$$

$$J = \rho_{atm} \frac{(q_l - q_s)}{1/g_s + r_b} \quad (\text{Eq 2b})$$

$$q_l = \exp\left(\frac{w \cdot LWP \cdot V_{H2O}}{R \cdot T}\right) \cdot q_{sat} \quad (\text{Eq 2c})$$

$$E = LA \cdot J \quad (\text{Eq 2a})$$

$$J = \rho_{atm} \frac{(q_l - q_s)}{1/g_s + r_b} \quad (\text{Eq 2b})$$

$$q_l = \exp\left(\frac{w \cdot LWP \cdot V_{H2O}}{R \cdot T}\right) \cdot q_{sat} \quad (\text{Eq 2c})$$

246 where E is the total transpiration of a tree, LA is the total leaf area (m^2), J is the transpiration per
 247 unit leaf area ($\text{kg s}^{-1} \text{m}^{-2}$), ρ_{atm} is the density of atmospheric air (kg m^{-3}), q_l is the
 248 within-leaf specific humidity (kg kg^{-1}), q_s is the atmosphere specific humidity (kg kg^{-1}),
 249 g_s is the stomatal conductance per leaf area, r_b is the leaf boundary layer resistance (s m^{-1}),
 250 w is a scaling coefficient (unitless), which can vary between 1 and 7, and here we use a value
 251 of 3; LWP is the leaf water potential (Mpa), V_{H2O} is the molar volume of water ($18 \times 10^{-6} \text{m}^3$
 252 mol^{-1}), R is the universal gas constant, and T is the leaf temperature (K).

253 The sap flow from absorbing roots to the canopy through each compartment of the tree
 254 along the flow pathway (absorbing roots, transport roots, stem, and leaf) is computed

255 according to Darcy's law in terms of the plant sapwood water conductance, the water potential
 256 gradient:

$$257 \quad Q_i = -K_i [\rho_w g(z_i - z_{i+1}) + (\Psi_i - \Psi_{i+1})] \quad Q_i = -K_i [\rho_w g(z_i - z_{i+1}) + (\Psi_i - \Psi_{i+1})]$$

258 (Eq 3)

259 where ρ_w is the density of water; z_i is the height of the compartment(m); z_{i+1} is
 260 the height of the next compartment down the flow path (m); Ψ_i is the water potential of the
 261 compartment(Mpa); Ψ_{i+1} is the water potential of the next compartment down the flow
 262 path(Mpa); and K_i is the hydraulic conductivity of the compartment ($\text{kg Mpa}^{-1} \text{m}^{-1} \text{s}^{-1}$). The
 263 hydraulic conductivity of the compartments is by the water potential and maximum hydraulic
 264 conductivity of the compartment through the pressure-volume (P-V) curve and the vulnerability
 265 curve (Manzoni et al. 2013, Christoffersen et al. 2016).

266 The plant hydrodynamic representation and numerical solver scheme within FATES-
 267 HYDRO follows Christoffersen et al. (2016). We made a few modifications to accommodate the
 268 multiple soil layers and to improve the numerical stability. First, to accommodate the multiple
 269 soil layers, we have sequentially solved the Richards' equation for each individual soil layer,
 270 with each layer-specific solution proportional to each layer's contribution to the total root-soil
 271 conductance. Second, to improve the numerical stability, we have an option to linearly
 272 extrapolate the PV curve beyond the residual and saturated tissue water content to avoid the rare
 273 cases of overshooting in the numerical scheme under very dry or wet conditions. Third,
 274 Christoffersen et al. (2016) use three phases to describe the PV curves: 1) dehydration phases
 275 representing capillary water (sapwood only), 2) elastic cell drainage (positive turgor), and 3)
 276 continued drainage after cells have lost turgor. Due to the possible discontinuity of the curve
 277 between these three phases, it leads to the potential for numerical instability. To resolve this
 278 instability, FATES-HYDRO added the Van Genuchten model (Van Genuchten 1980, July and
 279 Horton 2004) and the Campbell model (Campbell 1974) as alternatives to describe the PV
 280 curves.

281 In this study, we use the Van Genuchten model because of two advantages: 1) it is simple,
 282 with only three parameters needed for both curves, and 2) it is mechanistically based, with both
 283 the P-V curve and vulnerability curve derived from a pipe model, and thus connected through
 284 three shared parameters:

$$\Psi = \frac{1}{-\alpha} \cdot \left(\frac{1}{Se^{1/m}} - 1 \right)^{1/n} \quad (\text{Eq 4a})$$

$$FMC = \left(1 - \left(\frac{(-\alpha \cdot \Psi)^n}{1 + (-\alpha \cdot \Psi)^n} \right)^m \right)^2 \quad (\text{Eq 4b})$$

$$\Psi = \frac{1}{-\alpha} \cdot \left(\frac{1}{Se^{1/m}} - 1 \right)^{1/n} \quad (\text{Eq 4a})$$

$$FMC = \left(1 - \left(\frac{(-\alpha \cdot \Psi)^n}{1 + (-\alpha \cdot \Psi)^n} \right)^m \right)^2 \quad (\text{Eq 4b})$$

287 where Ψ is the water potential of the media (xylem in this case) (Mpa); FMC is the
 288 fraction of xylem conductivity, K/K_{\max} , (unitless); α is a scaling parameter for air entry point
 289 (Mpa^{-1}), Se is the dimensionless standardized relative water content as $Se = (\theta - \theta_r) / (\theta_{sat} - \theta_r)$
 290 expressed as $Se = (\theta - \theta_r) / (\theta_{sat} - \theta_r)$ with θ , θ_r , θ_{sat} are volumetric water content (m^3
 291 m^{-3}), residual volumetric water content, and saturated volumetric water content correspondingly;
 292 and m and n are dimensionless (xylem conduits) size distribution parameters. The model assumes
 293 that xylem conductance can be restored as xylem water content increases due to increased water
 294 availability after a dry period without any hysteresis in the FMC curve.

295

296 The stomatal conductance is modelled in the form of the Ball-Berry conductance model
 297 (Ball et al. 1987, Oleson et al. 2013, Fisher et al. 2015):

298
299

$$g_s = b_{slp} \frac{A_n}{c_s / P_{atm}} \frac{e_s}{e_i} + b_{opt} \beta_t g_s = b_{slp} \frac{A_n}{c_s / P_{atm}} \frac{e_s}{e_i} + b_{opt} \beta_t$$

(Eq 5)

300
301
302
303
304
305
306
307

where b_{slp} and b_{opt} are parameters that represent the slope and intercept in the Ball-Berry model, correspondingly. These terms are plant strategy dependent and can vary widely with plant functional types (Medlyn et al. 2011). The parameter b_{opt} is also scaled by the water stress index β_t . A_n is the net carbon assimilation rate ($\mu\text{mol CO}_2 \text{ m}^{-2} \text{ s}^{-1}$) based on Farquhar's (1980) formula. This term is also constrained by water stress index β_t in the way that the $V_{\text{cmax},25}$ is scaled by β_t as $V_{\text{cmax},25}\beta_t$ (Fisher et al. 2018). c_s is the CO_2 partial pressure at the leaf surface (Pa), e_s is the vapor pressure at the leaf surface (Pa), e_i is the saturation vapor pressure (Pa) inside the leaf at a given vegetation temperature when $A_n = 0$.

308
309
310

The water stress index β_t , a proxy for stomatal closure in response to desiccation, is determined by the leaf water potential adopted from the FMC_{gs} term from Christoffersen et al. (2016):

311
312

$$\beta_t = \left[1 + \left(\frac{\Psi_l}{P50_{gs}} \right)^{a_{gs}} \right]^{-1} \beta_t = \left[1 + \left(\frac{\Psi_l}{P50_{gs}} \right)^{a_{gs}} \right]^{-1}$$

(Eq 6)

313
314
315
316
317
318
319
320
321
322

where Ψ_l is the leaf water potential (MPa), $P50_{gs}$ is the leaf water potential of 50% stomatal closure, and a_{gs} governs the steepness of the function. For a given value of a_{gs} , the $P50_{gs}$ controls the degree of the risk of xylem embolism (Christoffersen et al. 2016, Powell et al. 2017). A more negative $P50_{gs}$ means that, during leaf dry down from full turgor, the stomatal aperture stays open and thus allows the transpiration rate to remain high and xylem to dry out, which thus can maintain high photosynthetic rates, at the risk of exposing xylem to embolism and thus plant mortality. Conversely, a plant with a less negative $P50_{gs}$ will close its stomata quickly during leaf dry down, thus limiting transpiration and the risk of xylem embolism and mortality associated with it, at the cost of reduced photosynthesis.

323 2.2.2 Sensitivity analysis and ~~Parameterization~~parameterization

324 The goal of this analysis is to better understand how coordinated aboveground and
325 belowground hydraulic traits determine plant physiological dynamics and the interplay between
326 ecosystem fluxes and tissue moisture during the extreme 2012-2015 drought at the Soaproot site.
327 We thus conduct a global sensitivity analysis on selected hydraulic parameters to explore the
328 linkages of aboveground and belowground hydraulic strategies. We use a full-factorial design for
329 the parameter sensitivity analysis in order to best investigate the relationships between
330 parameters. Because this design requires a relatively small set of parameters or groups of
331 parameters to vary, we chose parameters that represent the major axes of relatively well-
332 understood stomatal, xylem and rooting mechanisms/strategies that control the hydraulic
333 functioning of trees. We set the values of these parameters within the realistic (allowable
334 biological) range based on online database, and literatures where the species and physical
335 environment are as close to our system as possible. We list other major parameters and their
336 estimates that are not varied in the sensitivity analysis (table 2). We acknowledge that the biggest
337 disadvantage of this study is the lack of sufficient field data to constrain the model. This is a
338 result of using a natural drought as an experiment of opportunity, which, because it was not
339 anticipated, did not allow for ~~as~~ coordinated planning as would be the case in an experimentally-
340 manipulated drought. The trees at that site had all died by the time we started this study.

341 The parameters that we vary here are 1) the pair of r_a and r_b , which control vertical root
342 distribution as deep vs shallow roots, 2) two sets of xylem parameters (P_{50x} , K_{max} , m , n , and α)
343 that jointly represent two distinct xylem strategies: efficient/unsafe and inefficient/safe xylem
344 within the range observed for temperate conifer trees, and 3) the stomatal parameter $P50_{gs}$, which
345 represents the stomatal strategy along a risky to safe gradient (Table 1). The ranges of root
346 parameters are chosen so that the effective rooting depth, above which 95% of root biomass
347 stays, varies from 1m to 8m which is the possible range at the Soaproot site, as indicated by
348 current knowledge of the subsurface structure (see Klos et al., 2017). Note, here we refer to a
349 higher proportion of roots in deep subsurface layers as ‘deep rooting’ (e.g effective rooting depth
350 = 8m; $r_a=0.1, r_b=0.1$) as compared to ‘shallow rooting’ (e.g effective rooting depth = 2; $r_a=1, r_b=5$)
351 which represents a larger proportion of fine roots in upper layers (Figure 1a).

352 The safety-efficiency tradeoff of xylem has been widely discussed in the literature (e.g.
353 Gleason et al. 2016; Hacke et al. 2006, 2017; Martinez-Vilalta, Sala, and Piol 2004). Given that
354 we don't have any measurements that can be used to generate a vulnerability curve at our study
355 site, we consult the literature (Domec et al. 2004, Barnard et al. 2011, Corcuera et al. 2011,
356 Anderegg and Hillerislambers 2016, Baker et al. 2019, Kilgore et al. 2021) for observed curves
357 from sites that are as similar both in climate (e.g. mean annual precipitation and temperature) and
358 in the set of conifer species (*P. Ponderosa*) to our study site as possible, as well as values of
359 xylem traits (K_{max} and $P50_x$) of *Ponderosa* pine in temperate regions of the TRY database (Kattge
360 et al. 2020) to determine the two hypothetical vulnerability curves representing the
361 safe/inefficient and unsafe/efficient xylem strategies. We set the parameters of the van
362 Genuchten model to represent these two sets of P-V and vulnerability curves as shown in Fig 1b
363 and 1c. It is worth noting that with the same K_{max} and $P50$, the exact shape of the vulnerability
364 can differ depending on the formula used and parameter values. However, this should not be an
365 issue in our study because the vulnerability curve is mainly constrained by $P50$ and K_{max} .
366 Second, given that there is a large range of variation in the measured values, the effect caused by
367 the exact shape of the curves is minor. Third, since the objective of our study is not to accurately
368 predict mortality, but rather to examine the effect of different ~~combination~~combinations of
369 stomata, xylem, and root strategies, even if the shape of our vulnerability curve is not the most
370 accurate, as long as the curve captures the overall pattern of the pressure-conductivity relation, it
371 will not affect the relative outcome of this study.

372 We follow the theory of Skelton et al. (2015) to define safe vs. efficient stomatal strategy.
373 In FATES-Hydro, there are two key stomatal parameters: $P50_{gs}$ and a_{gs} . Here, we only vary
374 $P50_{gs}$ while keeping a_{gs} as a constant because the objective here is to choose the parameters that
375 are relatively well understood and to catch the safe vs. risky strategies as described by Skelton et
376 al., (2015) rather than ~~to~~ exhaust the parameter space within the model. In essence, the different
377 combinations of $P50_{gs}$ and the shape parameter (a_{gs}) can generate similar stomatal response
378 curves. For example, a small negative $P50_{gs}$ with a small a_{gs} would result in a flat stomatal
379 response curve, which is similar to a large negative $P50_{gs}$ combined with a large a_{gs} . Further,
380 $P50_{gs}$ is well understood and has more observed data, while a_{gs} is less studied and barely has any
381 observed data. With a given a_{gs} , the variance of $P50_{gs}$ for a given P_{xylem} value, controls the
382 degree of embolism risk, from a 'risky' strategy, where $P50_{gs}$ is equal to or lower than

383 P_{xylem} , to a ‘conservative’ strategy, where $P50_{gs}$ is higher than P_{xylem} . The P_{xylem} s in Skelton et
384 al.’s (2015) are for Fynbos species, therefore are not appropriate for our study because our
385 species are pine trees, a woody plant. Trees have woody tissue, which ~~contribute~~contributes to
386 ~~strengthen~~strengthening the conduits and ~~make~~makes them less ~~easy~~likely to collapse when
387 embolized, hence allow their stomata to be riskier than those of herbaceous plants. From the
388 observed $P50_{gs}$ and xylem traits of closely related pine species in the TRY database (Kattge et al.
389 2020) and elsewhere in the literature (Bartlett et al. 2016), as well as the observed soil water
390 potential at the study site, we choose to vary $P50_{gs}$ between $P50_{xylem}$ and $P20_{xylem}$,
391 (correspondingly the point at which xylem have lost 50% and 20% of their maximum
392 conductivity).

393 The emergent behavior of FATES or any model with dynamic ecosystem structure can
394 make analysis of physiological rate variation difficult, as the stand structure will respond and
395 thus also vary when parameters are changed. Here, we ~~wanted~~want to first understand the direct
396 trait control in the absence of structural differences. To overcome ~~complication~~complication of
397 the dynamic structure, we use a reduced complexity configuration for running the model which
398 we refer to as ‘static stand structure’ mode. To investigate dynamic competitive effects when
399 growth and mortality will be the next step. In this mode, the stand structure is initialized from
400 observed forest census data, and subsequently is fixed, i.e. the model does not permit plant
401 growth or death to change the vegetation structure. This allows the direct assessment of
402 hydraulic and physiological parameter variation in the model without the consequent feedback
403 loops associated with varying ecosystem structure. The stand structure is initialized with census
404 data from the CZ2 site (Table S1) and thus includes multiple cohorts of different sized trees.
405 Because this type of model configuration ignores prognostic plant mortality, in the interest of
406 being able to compare across simulations where mortality rates might otherwise be very high, we
407 use the loss of xylem conductivity as a measure of mortality risk of conifer trees at CZ2, which
408 has widely been used as an indicator of drought mortality of forest (e.g. Hammond et al., 2019).

409 To force the model with an atmospheric upper boundary, we use the Multivariate Adaptive
410 Constructed Analogs (MACA) climate data (Abatzoglou and Brown 2012) from 2008 – 2015 of
411 a 4km x 4km grid covers the study area. The daily average MACA data are disaggregated to 3-
412 hourly climate data (see Appendix S2 in Buotte et al. 2018 for detail). We set the initial soil

413 water content to be 75% of saturated water content, close to field capacity. We believe this is a
414 realistic value because the model is initialized in ~~Jan~~Januaryuary, when the study area has high
415 precipitation and trees are all in a dormant status, and in a year when there is not drought. We
416 also tried to initialize the soil with higher water content (e.g. saturation), but did not find any
417 ~~differences, -differences,~~as the extra water drained quickly in the winter when transpiration is
418 low.

419 3. Results

420 3.1 Sensitivity of GPP and ET to parameter perturbations

421 The parameter sensitivity analysis ~~shows~~revealed that in a monthly -mean flux
422 comparison, the simulations with deep roots ~~give~~provided a better match to the overall observed
423 pattern of the GPP and ET (~~Fig.~~Figure 2). ~~The~~In general, the simulated transpiration ~~contributes~~
424 ~~to~~contributed 90% of the ET ~~in general~~. The deep-rooted cases ~~better capture~~more accurately
425 ~~captured~~ the seasonality (e.g., the peak time) and the declining trend of observed GPP from
426 2011 to 2015. The deep-rooted cases also ~~match fairly well~~matched the observed ET fairly well.
427 The simulated GPP of shallow-rooted cases ~~are~~was higher than the observed values during wet
428 seasons (Dec. to Mar.~~),~~) but much lower than ~~the observed values~~those during the dry season of
429 the ~~pre-drought~~predrought period. ~~The~~Overall, the simulated ET of shallow-rooted cases ~~are~~
430 ~~overall~~was lower than the observed values. To quantify this assessment, we computed Root
431 ~~Mean-Square-Error (the~~ RMSE) from the hourly mean GPP and ET of each month and each year
432 of all ~~the~~40 cases (~~Fig.~~Figure S2). We ~~choose~~chose the RMSE as it is a common and compact
433 metric ~~offor~~ assessing model performance, though we note that other metrics could in principle
434 be used, each of which has different advantages and disadvantages (e.g., Collier et al., 2018).
435 The RMSE of the GPP and ET ~~decreases~~decreased with both effective rooting depth and P50gs
436 for both xylem strategies (~~Fig.~~Figure 3). The P50gs ~~has~~had less of an impact on the RMSE of the
437 GPP for the case with safe xylem than on that of the GPP for the case with efficient xylem. In
438 terms of the GPP, the effective rooting depth of 6.5m ~~gives~~5 m provided the best fit, as indicated
439 by the darkest color (GPP RMSE ~~of~~GPP= 1.12gC/m²/s, ET RMSE ~~of~~ET= 250 W/m²);
440 ~~under~~scoring). This underscores the importance of deep roots in maintaining transpiration and
441 photosynthesis during the dry season, as well as the role of deep roots in increasing the relative
442 decline in these fluxes during ~~the drought~~droughts.

443 Among the parameters that we varied in the sensitivity analysis, the vertical root
444 distribution has had the largest impact on the GPP and ET at CZ2. Figures Figure 2a-2b-b show
445 the monthly mean GPP and ET of the end members of the sensitivity analysis (see Fig-Figure S1
446 for the complete set of outcomes). We acknowledge that the variation in rooting depth across the
447 ensemble is was large, but point out; however, we also highlight that so is too was the uncertainty
448 in plant rooting depth, and moreover also that the uncertainty in rooting depth is was less well-
449 quantified than other plant traits such as (e.g., P50_z), such that this wide variation reflects a real
450 and deep uncertainty in plant rooting profiles. Deep roots result resulted in a substantially higher
451 GPP and transpiration during normal years (2011 and 2012). During long-term droughts, when
452 deep soil moisture is was depleted, the relative advantage of deep roots over shallow roots is was
453 reduced. Shallow roots result resulted in a substantially lower GPP and transpiration during the
454 dry season (Aug. to Oct.), with the seasonal maximum occurring earlier, in May; as
455 compared opposed to July with the deep-rooted cases. The shallow-rooted cases also have had a
456 much lower GPP and ET during the dry seasons of the pre-drought predrought period. During the
457 late stages stages of drought (2014 and 2015), the GPP and ET of the different cases
458 become became more similar between the shallow- and deep-rooted cases.

459 The second most important set of parameters in importance to rooting depth for controlling
460 carbon and water fluxes is are those that govern the stomatal strategy. The simulations with a
461 more risky riskier strategy ($P50_{gs} = P50_x$) gives provided a higher GPP and ET than the
462 simulation those with a safer strategy ($P50_{gs} = P20_x$) during pre-drought predrought periods and
463 the early stage of the drought (2011 to 2013), but they provided a slightly lower GPP and ET at in
464 the late stage of the drought (2014 and 2015) for the deep-rooted cases. However, risky stomata
465 gives provided a slightly higher GPP and ET at all times for shallow-rooted cases. The xylem
466 strategy has had the smallest effect on the GPP and ET of the parameters that we varied (e.g., the
467 the RMSEs of ET are were both around approximately $260 \text{ W/m}^2\text{m}^2$ for safe and efficient xylem, and
468 respectively, with $P50_{gs} = P20_x$ and 8 man effective rooting depth of 8 m). In deep-rooted cases,
469 the safe xylem and efficient xylem strategy result strategies resulted in an almost the
470 same identical GPP and ET, which can be seen via in the wides widest overlap between the dashed
471 and solid lines in figure Figure 1. In shallow-rooted cases, with safe stomata, safe xylem
472 generates generated a slightly higher GPP and ET than efficient xylem. In addition, the strength
473 of the effects of stomatal and xylem strategy strategies also depend on the rooting depth. The

474 deeper the effective rooting depth, the less significant the impacts of stomatal strategy
475 (~~Fig.~~Figure S1).

476

477 3.2 Sensitivity of plant water status to parameter perturbations

478 We ~~examine~~examined the impact of vertical root distributions, ~~and~~ stomatal and xylem
479 strategies on the seasonal variation of ~~the following~~ three plant ~~physiologic~~physiological
480 variables ~~that serve, which served~~ as indices of plant water stress (~~fig.~~Figure 4): the fraction loss
481 of xylem conductivity of ~~the~~ stem (SFL), leaf water potential (LWP), and an overall absorbing
482 root water potential (AWP). In the model, absorbing roots in different soil layers ~~have had~~
483 different water potentials, associated with the soil water potential of that layer. We
484 ~~calculate~~calculated a cohort-level effective AWP as the root-fraction--weighted average of water
485 potential in absorbing ~~root~~roots across all soil layers. ~~In this way~~Thus, the AWP represents the
486 overall rhizosphere soil moisture condition that is sensed by the tree. These physiological
487 variables ~~are were~~ tracked for each cohort. ~~For~~In any given case, the differences in these variables
488 among differently -sized cohorts ~~are were~~ negligible (~~Fig.~~Figure S3). Therefore, we present the
489 outcome of all ~~cohorts~~ cohorts with a diameter at breast height (DBH) between 50 ~~–60~~and 60
490 cm, the size class that ~~is was~~ most abundant at CZ2.

491 Stomatal and rooting strategies together ~~control~~controlled the loss of xylem conductivity
492 during the dry season of the ~~pre-drought~~predrought period and the whole period of the long-term
493 drought (~~Fig~~Figure 4a). In all cases, the xylem conductivity ~~reaches~~reached a maximum during
494 the wet season (Dec. to Jan.), ~~starts~~started to decline during the growing season (Apr. to Jun.),
495 ~~and~~ then ~~reaches~~reached its minimum in the dry season. With the same stomatal strategy, deep
496 roots ~~lead led~~ to a less -extreme loss of xylem conductivity than shallow roots. A deep rooting
497 strategy ~~is was~~ also able to maintain xylem conductivity with very little seasonal loss during the
498 ~~pre-drought~~predrought period, ~~but; however,~~ as deep soil moisture ~~is was~~ depleted, this effect
499 ~~is was~~ reduced. With a shallow rooting profile, the xylem conductivity ~~starts~~started to decline
500 earlier, and the minimum ~~is was~~ much lower than that of a deep rooting profile. For example,
501 with risky stomata, the minimum fraction of xylem conductivity ~~of in~~ deep-rooted cases in 2012
502 ~~is was~~ 0.4, but ~~is it was~~ lower than 0.2 with shallow roots. Unlike deep-rooted cases, ~~in shallow-~~
503 ~~rooted cases,~~ the seasonal variation of the loss of xylem conductivity ~~does did~~ not differ too much

504 during ~~pre-drought~~predrought and drought periods. ~~During the~~ in shallow-rooted cases.
505 Furthermore, during the very late stage of the drought, deep-rooted cases ~~have had~~ a lower
506 fraction of xylem conductivity than shallow-rooted cases (e.g., ~~in~~ in Jan. 2015).

507 In general, risky stomata ~~allow~~allowed a greater loss of xylem conductivity (K/K_{max}) than
508 safe stomata, but the extent ~~depends~~depended on the vertical root distribution. The effect of ~~the~~
509 stomatal strategy ~~is~~was more obvious in shallow-rooted cases. Risky stomata combined with
510 shallow roots ~~result~~resulted in ~~increasing an~~ increase in the duration of ~~the~~ 50% loss of xylem
511 conductivity, as well as the maximum loss of xylem conductivity during the dry season. With a
512 deep rooting strategy, the difference in the percentage loss of xylem conductivity between safe
513 ~~stomatal~~ and risky stomatal cases ~~increases~~increased with the progression of the drought, ~~but,~~
514 however, with a shallow rooting strategy, this difference ~~remains more or less~~remained
515 approximately the same over time. In addition, in 2011, a very wet year, with deep roots, a safe
516 xylem strategy ~~is~~was able to maintain the maximum xylem conductivity even during ~~the~~ dry
517 season (~~Fig~~Figure 4a). The impact of ~~the~~ xylem strategy on the percentage loss of xylem
518 conductivity ~~is~~was relatively weak. ~~For~~In both deep- and shallow-rooted cases, trees with safe
519 xylem ~~lose~~lost less xylem conductivity during the wet season but ~~lose~~ more conductivity during
520 the dry season.

521 The safe stomata ~~&~~and safe xylem cases for both deep- and shallow-rooted trees
522 ~~experience~~experienced greater declines in stem conductivity ~~as compared to~~with the safe stomata
523 and efficient xylem for the corresponding rooting depths (~~Fig~~Figure 4a). This is because with
524 safe stomata, trees operate at the right end of the vulnerability curve ~~shown~~displayed in
525 ~~fig~~Figure 1b, where the hydraulic conductivity of efficient xylem is much higher than that of ~~the~~
526 safe xylem. Thus, when ~~transpiring~~ the same amount of water, ~~the~~ is transpired, efficient xylem
527 will lose less water potential ~~as compared to~~than safe xylem. This keeps the xylem water
528 potential of a plant with efficient xylem higher than ~~that of~~ one with safe xylem, and
529 consequently, it also keeps the xylem conductivity, K , higher. This is also because we set $P_{50_{gs}}$
530 based on P_{xylem} ; thus, the $P_{50_{gs}}$ of safe stomata for plants with efficient xylem ~~is~~was higher (less
531 negative) than that of plants with safe xylem, ~~thus~~ resulting in lower transpiration rates, which in
532 ~~term~~ reduces ~~turn~~ reduced the loss of xylem water potential. As a result, plants with both safe
533 stomata and efficient xylem not only ~~transpire~~transpired less water but also ~~lose~~lost less water

534 potential per volume of ~~transpired~~ water ~~transpired~~. Together, these two mechanisms
535 ~~contribute~~~~contributed~~ to ~~keep~~~~keeping~~ the xylem conductivity of the efficient xylem cases higher.

536 ~~Stomata~~~~In addition, stomatal~~, rooting, and xylem strategies ~~have~~~~had~~ similar impacts on
537 the seasonal variation of both leaf and fine root water potentials (~~Fig4e~~~~Figure 4c~~ and 4d). Leaf
538 and fine root water potentials ~~peak~~~~peaked~~ during the winter, then ~~start~~~~started~~ to decline in early
539 spring~~s~~, and ~~reach~~~~reached~~ their lowest point in the dry season. Deep roots, safe stomata, and safe
540 xylem traits all ~~contribute~~~~contributed~~ to the maintenance of higher leaf and fine root water
541 potentials during the growing and dry seasons. With deep roots, there ~~is~~~~was~~ less ~~of a~~ difference
542 in leaf and fine root water ~~potential~~~~potentials~~ between stomatal and xylem strategies in the very
543 wet year ~~of~~ 2011. Plants that combine safe stomata and/or safe xylem with deep roots ~~can~~~~were~~
544 ~~able to~~ keep the leaf and fine root water potentials relatively high (less than -5 Mpa) during the
545 dry season of the drought period. However, while plants that combine risky stomata or efficient
546 xylem with deep roots ~~can~~~~could~~ keep the dry season leaf water potential above -5 Mpa during the
547 ~~pre-drought~~~~predrought~~ period, their traits ~~lead~~~~led~~ to the dry season leaf water potential dropping
548 below -8 Mpa or even ~~below~~-10 Mpa during the drought period. In both deep-~~rooted~~ and
549 shallow-rooted cases, safe xylem ~~leads~~~~led~~ to much lower leaf and fine root water potentials
550 during the dry season. The seasonal and inter-annual variation of fine root water potentials
551 ~~are~~~~was~~ almost identical to the leaf water potential, except that the water potential of fine roots
552 ~~is~~~~was~~ slightly higher (~ 0.5 Mpa) than the leaf water potential.

553 3.3 Sensitivity of subsurface hydrology to parameter perturbations

554 In the simulation outcomes, the vertical root distributions again ~~have~~~~had~~ the largest impact
555 on ~~hydrologie~~~~hydrological~~ processes ~~and~~, subsurface water content, and ~~the way that~~~~how~~ they
556 ~~change~~~~changed~~ over the drought. With deep roots, there ~~is~~~~was~~ less drainage loss from surface
557 and subsurface runoff ~~as~~ compared ~~to~~~~with~~ shallow roots, especially during the growing season
558 (Figure 5a, c, e, ~~and~~ g). The subsurface water content ~~show~~~~exhibited~~ different vertical and
559 temporal patterns between the cases with different vertical root distributions. In the deep-rooted
560 cases, during the ~~pre-drought~~~~predrought~~ period, the water content in the deepest layers
561 ~~fluctuates~~~~fluctuated~~ between wet and dry ~~seasonally~~~~seasons~~; during the first year of the drought,
562 the water content of the deepest layers (6 ~~to~~ 8 ~~m~~ 8 m) slightly ~~increases~~~~increased~~ during the wet
563 season, but ~~with the progression of~~ ~~as~~ the drought ~~progressed~~, the soil water content

564 ~~becomes~~became consistently depleted in the middle and deep layers (~~between 5 and 8 m depth~~)
565 and only the shallow ~~layer~~layer's (<0.16 m) water content ~~increases~~increased during ~~the~~ wet
566 season. In the shallow-rooted cases (Figure 5b, d, f, ~~and~~ h), soil moisture in the surface layers
567 (top ~~2 m~~)~~shows 2 m~~ exhibited seasonal variation, but this ~~seasonal variation becomes~~became
568 weaker ~~over with~~ depth ~~and~~. Moreover, the soil moisture at ~~6-8 m~~ 8 m depth ~~stays~~stayed
569 consistently high throughout the year during ~~pre-drought~~the predrought period; and
570 ~~remains~~remained slightly low ~~through~~throughout the entire drought period; while the water
571 content of the middle and upper layers of the shallow-rooted case ~~have~~exhibited a similar pattern
572 of seasonal variation before and during the drought.

573 ~~Stomata!~~The stomatal strategy, as quantified by $P50_{gs}$, ~~has~~had a weak impact on
574 ~~hydrologie~~hydrological processes and soil moisture. In both ~~the~~ deep- and shallow-rooted cases,
575 riskier stomata ~~lead~~led to a slightly lower total subsurface water content (Figure 6a). The effect
576 of $P50_{gs}$ ~~is~~was less significant during the ~~pre-drought~~predrought period for both the deep- ~~and~~
577 ~~shallow-rooted cases~~ and ~~shallow-rooted cases, and becomes~~became more significant as the
578 drought ~~progresses~~progressed. The effect of $P50_{gs}$ on total subsurface water content ~~is~~was less
579 significant in shallow-rooted cases. Figure 5c ~~shows~~presents the effect of $P50_{gs}$ on the water
580 content of shallow and deep soil layers. In both the shallow- and deep-rooted cases, increasing
581 $P50_{gs}$ ~~has~~had a negligible impact on the water content of the shallow layers during both the ~~pre-~~
582 ~~drought~~predrought and drought periods (Figure 5c, left). For deeper layers, in the shallow-rooted
583 case, $P50_{gs}$ ~~has~~had no impact on the water content at ~~all times any time~~; in the deep-rooted cases,
584 a risky $P50_{gs}$ ~~results~~resulted in a lower dry season water content of deep layers (~~7-8 m~~ 8 m)
585 during the ~~pre-drought~~predrought period (as indicated by the red cycles ~~of~~in Figure 5a and 5c),
586 but ~~decreases~~it decreased the water content of those layers year-round during the drought period
587 (Figure 5a and 5e). In deep-rooted cases, safe stomata with efficient xylem ~~lead~~led to a slightly
588 higher water content in deep layers (~~5 m to 8 m~~ 5-8 m) during the ~~pre-drought~~predrought period;
589 and in shallow layers (~~0 to 3 m~~ 3 m) during the drought period (Figure 6a). Risky stomata with
590 safe xylem in deep-rooted cases ~~are~~were most effective ~~in~~at accessing soil water.
591 ~~Though~~Although the soil water contents ~~are~~were generally high in shallow-rooted cases,
592 stomatal and xylem strategies ~~show~~exhibited a similar impact on ~~the~~ soil water storage as those
593 in ~~the~~ deep-rooted cases (FigFigure S4).

594 ~~Simulations~~ Furthermore, simulations with deep roots ~~have~~ resulted in almost no loss of
595 soil water to drainage during the dry season in normal years; or during the whole drought period;
596 ~~while~~ by contrast, in simulations with shallow roots, the drainage loss ~~is~~ was high during the ~~pre-~~
597 ~~drought~~ predrought period and ~~decreases~~ decreased through the drought period, but still with some
598 runoff even at the end of the ~~drought~~ period (Figure 6a). The observed total annual runoff from
599 the 2008 ~~to~~ 2011 ~~pre-drought~~ predrought period was ~~about~~ approximately 250 mm/year, but ~~it~~
600 was zero during the 2012—2015 drought period (from ~~figure~~ Figure 4,; Bales et al. 2018). This
601 observed difference in runoff between the ~~pre-drought~~ (~290mm) predrought (~290 mm/year,
602 2011—2012) and drought periods (~0 mm/year) ~~from~~ in the deep-rooted case ~~is~~ was consistent
603 with the predicted pattern. During the ~~pre-drought~~ predrought period, the wet season total
604 subsurface water contents from ~~Dec.~~ December to ~~Feb.~~ February were similar between the
605 cases with deep and shallow roots, ~~but~~; however, during the dry season (from June to Sep.) the
606 total subsurface water content with shallow roots ~~is~~ was substantially higher than the case with
607 deep roots (Figure 6b).

608 4. Discussion

609 4.1 Vertical root distribution as the first-order control

610 The ~~outcome~~ outcomes of our simulations ~~indicates~~ indicated that the vertical root
611 distribution ~~exerts the~~ exerted first-order control over both ecosystem-level fluxes and plant
612 physiology at CZ2. This dominance of ~~the~~ rooting strategy over other hydraulic traits is related to
613 the nature of the rainfall pattern ~~of~~ in the Mediterranean-type climate of that region. The CZ2 site
614 receives effectively all of its rain during ~~the~~ winter. This water is stored in the soil column and
615 slowly released through the growing season. The root zone soil moisture ~~has~~ exhibits strong
616 seasonal variation, which constrains plant water use and gas exchange as a function of the
617 gradual drying of the soil column (Bales et al., 2018). In the model, the stomatal behavior ~~is~~ was
618 controlled by the leaf water potential, which itself ~~is~~ was strongly affected by the root zone soil
619 moisture. In our simulations, the daytime average leaf water potential of a 55cm DBH cohort
620 ~~is~~ was well correlated with the fine root water potential and ~~is~~ was always ~~about~~ approximately 0.5
621 Mpa lower (~~fig~~ Figure S5). This offset is consistent with the relationship between ~~the~~ mid-day
622 leaf water potential and ~~pre-dawn~~ predawn leaf water potential found by Martínez-Vilalta et al.
623 (2014) at the global scale.

624 With deep roots, trees ~~use~~used more subsurface storage capacity at the CZ2 site, ~~and thus a~~
625 ~~higher amount of total rainfall.~~ In a wet ~~year~~years such as 2011, the root zone water potential of
626 deep-rooted trees ~~is kept~~was maintained relatively high (Figure 4b) and the trees ~~operate~~operated
627 at the upper end of their vulnerability curve ~~through~~throughout the year, with a typical loss of
628 conductivity ~~of~~ 10% (~~Fig~~Figure 7). Therefore, we ~~don't see~~did not observe much ~~of an~~
629 ~~the~~ stomatal strategy on ~~the~~ GPP and transpiration in a wet ~~year~~years. At the upper end of the
630 vulnerability curve, stomata ~~are~~were fully open regardless of ~~the~~ stomatal strategy (either ~~to be~~
631 safe or risky). When the drought began in late 2012, annual rainfall fell below the total root zone
632 storage, ~~thus~~and therefore, the deep storage remained depleted throughout the year. During the
633 drought, the deep-rooted trees were able to operate at the high end of the vulnerability curve in
634 the wet season, when the rainfall recharged the surface layer. As the surface layers ~~dry~~dried,
635 water potential then gradually ~~falls~~fell to the lower end of the vulnerability curve; consequently
636 ~~the~~, photosynthesis and transpiration ~~start~~started to drop as the dry season ~~progresses~~progressed.
637 With risky stomata, trees can drive ~~the~~ soil moisture to lower values. This is why we ~~see~~observed
638 the difference in the effect on ~~the~~ GPP and transpiration between different stomatal strategies
639 during the dry season ~~when~~as the drought ~~progresses~~progressed.

640 With shallow roots, trees can only use surface soil moisture storage. As a result, the
641 surface water storage ~~is~~was quickly used up after the wet season, and the root zone water
642 potential ~~drops~~dropped near the low end of the vulnerability curve during the dry season. Thus,
643 ~~the~~ shallow-rooted trees ~~operate~~operated along the full extent of the vulnerability curve year-
644 round, ~~both~~ during ~~the pre-drought~~both predrought and drought periods. Therefore, ~~as~~ for the
645 deep-rooted cases, we ~~don't see~~did not observe a strong effect of stomatal strategy on ~~the~~ GPP
646 and transpiration during the wet season, ~~but~~; however, unlike the deep ~~root-rooted~~
647 effect of stomatal strategy on ~~the~~ GPP and transpiration during the dry season ~~can~~could be
648 ~~seen~~observed throughout the whole simulation period.

649 Rooting strategies greatly control the spatial pattern of vertical soil water content (Figure
650 5). With deep roots, the vertical soil moisture variation ~~is~~was more homogeneous due to the
651 extensive root distribution. With shallow roots, the soil ~~becomes~~became extremely dry at the
652 surface (~~4m~~1 m) and extremely wet in deep layers (~~5m~~resulting from 5 m) ~~as a result of~~ the
653 aggregated root distribution in the upper layers. ~~Our~~This finding is similar to ~~a recent study~~

654 ~~conducted by that of~~ Agee et al. (2021), ~~where the authors who~~ found that ~~the~~ extensive lateral
655 root spreading results in homogeneous soil moisture distribution. The homogeneous soil
656 moisture pattern may contribute to a more energy-efficient system that reduces plant water stress
657 (Agee et al. 2021) because ~~that it~~ minimizes the loss of energy dissipation ~~loss~~ through water
658 transport (Hildebrandt et al. 2016). Both our study and that of Agee et al. (2021) ~~and our studies~~
659 emphasize the importance of the means by which the root distributions determine how the
660 subsurface storage is ~~utilized.~~ used.

661 Given the shape of the vulnerability curves, ~~in all these simulations,~~ plants will
662 ~~stop stopped~~ transpiring in all simulations when their leaf water potential ~~reaches around~~
663 ~~10Mpa reached approximately -10 MPa~~ with efficient xylem or ~~-15Mpa -15 MPa~~ with safe
664 xylem, depending on their stomatal strategy (FigFigure 7). Because we ~~are here holding held~~ the
665 stand structure and leaf area constant to allow ~~comparison comparisons~~ between cases, the
666 simulated leaf water potential of the shallow-rooted, risky stomata combination ~~can get could~~
667 reach as low as ~~-15Mpa -15 Mpa~~ (Figure 4b) during dry seasons, even during ~~pre-drought the~~
668 predrought period, which is well below the lowest possible leaf water potential observed (~~-~~
669 ~~10Mpa) (-10 Mpa;~~ Vesala et al., 2017). Leaves ~~will would~~ likely be wilted before the water
670 potential drops below ~~-10Mpa -10 MPa~~, and the tree would ~~have already~~ have shed the leaves
671 due to canopy desiccation. ~~But However,~~ we specifically ~~did did~~ not permit that ~~to occur~~ in these
672 simulations, ~~so as~~ to keep the different cases comparable. Although it might be unrealistic, the
673 leaf water potential can serve as an ~~indicator indicator~~ of the degree of canopy desiccation. With
674 no or very ~~little leaves few leaves~~, trees would rely on ~~the storage stored~~ carbon to support
675 respiratory demand until the wet season ~~comes arrives~~ to regrow leaves. Depending on the
676 duration of the dry season, trees may exhaust ~~the their~~ stored carbon and die from carbon
677 starvation. ~~Risky While risky~~ stomata can generate a higher GPP (Figure 1a), ~~but they~~ also result
678 in a longer duration of more negative leaf water potential (Figure 4b). This suggests that shallow-
679 rooted pines at CZ2 with risky stomata ~~will would~~ benefit from allocating more net primary
680 productivity to their storage pools rather than growth in order to reduce ~~the~~ carbon-starvation
681 mortality. Therefore, even though the model ~~generates generated~~ unrealistically low leaf water
682 potentials, the extent and ~~the~~ duration of ~~the these~~ simulated ~~very low leaf water potential~~
683 allows potentials allowed us to gain some ~~insight on insights into~~ the interaction of ~~plant plants'~~
684 hydraulic ~~strategy strategies~~ and the life history ~~strategy strategies~~ of conifer trees under a

685 Mediterranean-type climate. ~~Furthermore, Further,~~ the unrealistic leaf water potential from the
686 shallow root simulations ~~indicates~~indicated that the trees at that site must have ~~really~~very deep
687 roots to exist ~~at this site~~there, which is in agreement with the conclusions of Goulden and Bales
688 (2019).

689 In this simulation, the impacts of xylem traits on the GPP and ET ~~are~~were weak and subtle.
690 This ~~is~~was the result of the relative position of the two vulnerability curves, ~~in~~
691 ~~particular,~~particularly the intersection of the two vulnerability curves in absolute conductivity.
692 When the absolute conductivity ~~is~~was plotted as a function of pressure (~~fig.~~Figure 1b and solid
693 lines in ~~fig.~~Figure S6), ~~it can be seen that~~we observed, on the left side of the intersection, that the
694 safe xylem ~~is~~was not only safe but also efficient, ~~and; thus,~~ a safety-efficiency tradeoff of
695 xylem ~~thus~~ only ~~occurs~~occurred on the right side of the intersection point. Therefore, in shallow-
696 rooted cases, when the root zone water content—and hence the plant water status—is low, safe
697 xylem can generate a slightly higher GPP and ET than unsafe xylem. Furthermore, the two
698 pressure-conductivity curves ~~diverged~~diverged mainly at the wet end (corresponding to the wet
699 season). This is likely to be because the xylem structures of conifers are very similar, and the
700 range of variation of xylem traits in the sensitivity analysis ~~are~~was limited to the dominant
701 species at the site. Therefore, the difference in the xylem traits of conifers ~~do~~does not cause
702 significant impacts on the ecosystem-level fluxes under the Mediterranean-type climate of CZ2,
703 ~~where the ecosystem fluxes~~which are constrained by energy during the wet season (Goulden et
704 al., 2012). In addition, the maximum ~~rate~~rates of GPP and ET are co-constrained by the stand
705 density, ~~the~~ total leaf area, ~~the~~ maximum stomatal conductance, and VPD. In this study, we used
706 the static stand structure mode of FATES-Hydro, whereby the stand density and the total leaf
707 biomass (so as total leaf area) of the trees ~~are~~were held constant. This further ~~limits~~limited the
708 effect of xylem traits on the GPP and ET.

709

710 4.2 Balancing productivity and mortality risk

711 The hydraulic traits that contribute to high carbon fixation rates often make trees more
712 susceptible to drought. Stomatal strategy ($P_{50_{gs}}$) can have both positive and negative
713 ~~impact~~impacts on ~~the~~ trees, creating a tradeoff in the balance between productivity and
714 physiological stress. The risky stomata ($P_{50_{gs}} = P_{50_x}$) can generate a higher GPP but also result

715 in a greater loss of xylem conductivity and lower leaf water potential. The tradeoff varies
716 depending on the plant's root strategy—(i.e., having a deep vs. a shallow root distribution—)
717 and ~~the~~ moisture state.

718 To better understand the tradeoff between productivity and mortality risk, we ~~plot~~plotted
719 the simulated annual average GPP for each year against the fraction of conductivity (K/K_{max}) of
720 a ~~55 cm~~55 cm DBH cohort for two scenarios: — deep roots (Fig. Figure 8a) and shallow roots
721 (Fig. Figure 8b); — with different ~~combination~~combinations of xylem and stomatal strategies. In
722 both scenarios, for each pair of xylem and stomatal strategies, the GPP per tree
723 ~~increases~~increased almost linearly with ~~the~~ K/K_{max} . ~~But, with increasing~~However, as the safety
724 of the stomata increased, the GPP ~~declines~~declined faster with the loss of conductivity. This
725 response is stronger in deep-rooted scenarios. Having ~~efficient~~efficient xylem only slightly
726 ~~increases~~increased the steepness of the lines. The stomatal strategies thus ~~represent~~represented
727 points along a gradient of the tradeoff between growth and mortality risk—; the safer the stomata,
728 the more the GPP is traded ~~for reducing the to reduce~~ mortality risk.

729 Along this tradeoff space, ~~where~~the point at which trees can maximize their net carbon
730 gains likely depends on the xylem traits. Studies have ~~shown~~demonstrated that trees may
731 temporarily lose xylem conductivity during mild ~~drought~~droughts, which can recover once ~~the~~
732 soil water becomes available. However, under ~~an~~ extreme drought, their xylem could collapse
733 and permanently damage the xylem conduits. In this case, trees rely on new sapwood growth to
734 support ~~the~~ transpiration (Brodribb et al. 2010, Anderegg et al. 2013). At one extreme, if the
735 stomatal behavior is too safe, it will giveproduce a low GPP and the tree will be outcompeted for
736 light due to faster-growing neighbors, ~~but;~~ however, at the other extreme, if the stomata behave
737 very ~~aggressive~~aggressively (risky), ~~it~~this will giveproduce a high GPP but also empty the
738 subsurface storage quickly, consequently leading to a prolonged dry period of soil moisture. This
739 would lead to substantial xylem damage (and/or root death), and then the carbon ~~needed~~required
740 to grow new sapwood (or roots) ~~can~~could exceed the ~~benefit of getting~~benefits from the
741 additional GPP. ~~So~~Thus, the optimal location along the gradient would probably be located
742 slightly below the K/K_{max} associated with that critical xylem water potential. Currently, the
743 xylem refilling and associated carbon cost are not incorporated ~~in~~into FATES-Hydro. These two

744 processes should be implemented in the model to ~~better understand~~ obtain an enhanced
745 understanding of the water-carbon balance, ~~which, and thus~~ remains ~~as for~~ future work.

746 In the deep-rooted scenario, the values of the ~~pre-drought~~ predrought period and early
747 drought stage ~~are were~~ clustered ~~at in~~ the upper-right corner, above a K/K_{max} of 0.6. (~~Fig. (Figure~~
748 8a). In this region, the stress from the loss of xylem conductivity likely ~~won't~~ would not be high
749 enough to cause severe consequences, if ~~using we were to use a 50-percent~~ % loss of xylem
750 conductivity as the threshold for mortality and/or permanent xylem damage. The deep-rooted
751 tree can thus benefit by trading less GPP for maintaining xylem conductivity with a risky/more -
752 productive stomatal strategy during normal years. ~~But~~ However, during the late ~~stage~~ stages of the
753 drought (2014 and 2015), the conductivity values ~~become~~ became much lower. If this ~~mega~~
754 ~~drought~~ megadrought stopped earlier, (e.g., if it were a mild drought that only lasted for two
755 years), then the additional GPP obtained from risky stomata may ~~overweight~~ outweigh the
756 carbon cost ~~for of~~ repairing xylem damage. This suggests that, if the 2012—2015 drought was
757 not common in California, then natural selection might favor the risky/more -productive stomatal
758 strategy for deep-rooted trees. However, ~~this~~ the same strategy would also ~~exposes~~ expose trees to
759 a high mortality risk ~~under~~ during severe droughts.

760 In the shallow-rooted case (~~Fig. Figure~~ 8b), the values ~~are were~~ all clustered lower and to
761 the left, ~~as~~ compared ~~to with the~~ deep-rooted scenario, irrespective of the drought status. Thus, for
762 shallow roots, risky/more -productive stomatal behavior ~~results~~ resulted in a similarly high
763 mortality risk during both the ~~pre-drought~~ predrought and drought ~~period~~. ~~Thus~~ periods.
764 Accordingly, under the long-term climate conditions ~~seen~~ found at CZ2, regardless of whether ~~or~~
765 ~~not~~ severe droughts were frequent or not, the only shallow-rooted trees that could persist would
766 have to follow the safe and less-productive stomatal strategy. ~~And, thus~~ Therefore, safe and less-
767 productive stomata also ~~protects the~~ protect shallow-rooted ~~tree plant~~ trees from mortality risk
768 during drought.

769 The model outcome ~~indicates~~ indicated that under drier root zone soil conditions, if pines
770 were to follow a shallow rooting strategy, they would benefit from a safer stomatal strategy, with
771 more conservative water use; ~~but~~ by contrast, if they were to follow a deep rooting strategy,
772 ~~pinesthey~~ would benefit from riskier stomata. This is consistent with Anderegg et al.'s (2016)
773 finding ~~on~~ regarding the relative stomatal conductance (g_s) across elevation. They found that at a

774 low elevation (lower precipitation) site, Ponderosa pine ~~has had~~ lower relative stomatal
775 conductance and less loss of xylem conductivity, equivalent to safer stomata in our study, while
776 at a mid-elevation (higher precipitation) site, ~~pine has it had~~ higher relative stomatal conductance
777 and a greater loss of xylem conductivity, equivalent to risky stomata in our study. The simulation
778 results are consistent with the idea that the CZ2 region is dominated by deep-rooted trees. ~~This,~~
779 which is supported by previous studies. In situ measurements of regolith structure
780 (~~particularly particularly~~ the porosity) ~~indicates indicate~~ that at CZ2, there is a layer of thick,
781 semi-weathered ~~bedrock bedrock~~ that ~~allows allows~~ the trees to grow deep roots (Holbrook et al.,
782 2014). Growing deep roots to access rock moisture to support plant water use ~~has was also been~~
783 observed in the Eel River CZO catchment (Rempe et al., 2018), another Mediterranean-type
784 ecosystem along the west coast. Observed net CO₂ exchange and ET during the ~~pre-~~
785 ~~drought predrought~~ period ~~suggests suggested~~ that during a wet year, deep moisture supported
786 summer transpiration and productivity when the upper layer moisture was low (Goulden et al.
787 2015). Because the deep rooting strategy is sufficient in most cases ~~to avoid for avoiding~~ the main
788 effects of dry seasons and short droughts, and ~~that because~~, conditional on having deep roots, the
789 risky stomatal strategy confers a productivity advantage at a little increased risk of vulnerability,
790 ~~then~~ we would expect ~~that~~ plants with these traits ~~would to~~ dominate. However, under extreme
791 cases such as the 2012—2015 drought, which ranked as one of the most severe in California in
792 the last 1200 years (Lu et al. 2019), we would expect ~~that~~ plants with this deep-rooted, risky
793 stomatal strategy ~~would to~~ be highly vulnerable to drought, which is consistent with the
794 ~~~approximately~~ 90% mortality of the pine observed at CZ2 during the drought (Fettig et al.
795 2019). The water balance of the catchment based on ~~the~~ long-term observation from
796 precipitation, stream flow, and ET (Bales et al. 2018, Goulden and Bales 2019) also
797 ~~supports supports~~ that it was the slow depletion of deep moisture that caused tree mortality in the
798 late stage of the prolonged 2012—2015 drought.

799 The ~~finding findings~~ of our study ~~indicates indicate~~ that ~~the~~ future drought mortality
800 ~~would will~~ likely occur in ~~the~~ ecosystems ~~which that~~ are ~~eo-~~limited by water and other factors. In
801 ~~those such~~ ecosystems, trees can benefit from having more efficient but less safe hydraulic traits,
802 ~~which has they~~ allow them to be more competitive for water, and bring in a higher GPP. The extra
803 carbon gain can be used to develop measures ~~to deal for dealing~~ with other constraining factors,
804 such as ~~increase storage increasing stored~~ carbon to lower the risk of carbon starvation, ~~or~~

805 ~~build~~building thicker bark to resist fire, and ~~to grow~~growing more roots, which further enhance
806 their capacity to compete for water.

807 5. Conclusions

808 Our analysis indicates that root distribution can affect the most competitive stomatal
809 ~~stomatal~~ traits. ~~In~~In a Mediterranean-type climate where the supply of energy and water is
810 desynchronized and accessible subsurface water storage capacity is close to annual precipitation,
811 deep roots combined with risky stomata represent a beneficial strategy for high productivity in
812 normal years with low mortality risk, ~~but~~; however, this strategy exposes trees to a high
813 mortality risk during multi-year droughts. While such a strategy enables trees to fully ~~utilize~~use
814 subsurface storage and precipitation for productivity over ~~the~~ regular years, the lack of deep
815 water storage recharge during droughts exposes trees to high drought stress and makes this
816 strategy unfavorable under severe and prolonged drought. ~~In~~By contrast, shallow roots combined
817 with safe stomata represent a strategy for drought resistance, albeit at the cost of considerably
818 reduced productivity, as such a combination only allows trees to use shallow subsurface storage
819 while leaving deep moisture untouched; ~~thus~~, less precipitation is used for productivity.
820 ~~But~~However, this strategy leaves trees ~~to be~~ less susceptible to drought-induced mortality should
821 the deep reservoir be depleted. ~~By~~In contrast, shallow roots with risky ~~stoma~~stomata lead~~ta leads~~
822 to high mortality even during ~~non-drought year~~nondrought years, making this an s, thus
823 ~~an~~uncompetitive combination at the site. These results suggest that stomatal strategy is
824 controlled by root zone soil moisture and regulated by root distribution in that region. Thus, our
825 study underscores the importance of considering plant rooting and hydraulic strategies within the
826 larger context of plant ecological strategies.

827

828 Author contribution

829 JD and CDK design the study and write the MS. JD conducted the simulation. PB, RB, MG
830 provided model input data. BC, CDK, RF, RK, CX, and JD wrote the code. PB, RB, BC, RF,
831 MG, RK, LK, JS, CX edited the MS.

832

833 Acknowledgement

834 We acknowledge support by the Director, Office of Science, Office of Biological and
835 Environmental Research of the U. S. Department of Energy under Contract DE-AC02-
836 05CH11231 through the Early Career Research Program, the University of California Laboratory
837 Fees Research Program, and National Science Foundation Southern Sierra Critical Zone
838 Observatory grant EAR-1331931. RF acknowledges funding by the European Union’s Horizon
839 2020 (H2020) research and innovation program under Grant Agreement No. 101003536
840 (ESM2025 – Earth System Models for the Future) and 821003 (4C, Climate-Carbon Interactions
841 in the Coming Century)

842 **Data availability statement**

843 The FATES code (branch FATEScodeforMS1), parameter files and data that support the
844 findings of this study are openly available at ZENODO:
845 [https://zenodo.org/account/settings/github/repository/JunyanDing/Rooting-and-Hydraulic-](https://zenodo.org/account/settings/github/repository/JunyanDing/Rooting-and-Hydraulic-strategy-of-pine-at-Sierra-CZ2-)
846 [strategy-of-pine-at-Sierra-CZ2-](https://zenodo.org/account/settings/github/repository/JunyanDing/Rooting-and-Hydraulic-strategy-of-pine-at-Sierra-CZ2-) (DOI 10.5281/zenodo.5504405). The flux tower data can be
847 retrieved from the UC Merced online database (<https://www.ess.uci.edu/~california/>).

848 **Competing interests**

849 The authors declare no conflict of interest

850 5. References

- 851 Abatzoglou J.T. and Brown T.J. "A comparison of statistical downscaling methods suited for
852 wildfire applications" *International Journal of Climatology* (2012), 32, 772-780. 2012.
- 853 Adams, H. D. et al. "Mechanisms in Drought-Induced Tree Mortality." *Nature Ecology &*
854 *Evolution* 1(September). <http://dx.doi.org/10.1038/s41559-017-0248-x>. 2017.
- 855 Agee, E., He, L., Bisht, G., Couvreur, V., Shahbaz, P., Meunier, F. et al., 2021. Root lateral
856 interactions drive water uptake patterns under water limitation. *Adv. Water Resour.*, 151:
857 103896.
- 858 Anderegg, W.R., Plavcová, L., Anderegg, L.D., Hacke, U.G., Berry, J.A. and Field, C.B.,
859 Drought's legacy: multiyear hydraulic deterioration underlies widespread aspen forest die-
860 off and portends increased future risk. *Global change biology*, 19(4), pp.1188-1196. 2013.
- 861 Anderegg, L. D. L. and Hillerislambers, J. Drought stress limits the geographic ranges of two
862 tree species via different physiological mechanisms *Glob. Chang. Biol.* 22 1029–45
863 Online: <http://dx.doi.org/10.1111/gcb.13148> . 2016
- 864 Ando, Eigo, and Kinoshita, Toshinori. "Red Light-Induced Phosphorylation of Plasma
865 Membrane H⁺ -ATPase in Stomatal Guard Cells." *Plant Physiology* 178(October): 838–49.
866 2018.
- 867 Baker, Kathryn V., Tai, Xiaonan, Miller, Megan L, Johnson, D. M., Six co-occurring conifer
868 species in northern Idaho exhibit a continuum of hydraulic strategies during an extreme
869 drought year, *AoB PLANTS*, Volume 11, Issue 5, October 2019, plz056,
- 870 Bales, Roger et al. "Spatially Distributed Water-Balance and Meteorological Data from the Rain
871 – Snow Transition , Southern Sierra Nevada , California." : 1795–1805. 2018.
- 872 Bales, Roger et al. 2018. "Mechanisms Controlling the Impact of Multi-Year Drought on
873 Mountain Hydrology." *Scientific Reports* (December 2017): 1–8.
- 874 Ball, J. Timothy, Ian E. Woodrow, and Joseph A. Berry. "A model predicting stomatal
875 conductance and its contribution to the control of photosynthesis under different
876 environmental conditions." *Progress in photosynthesis research*. Springer, Dordrecht, 221-
877 224. 1987.
- 878 Barnard, DM, Meinzer, FC, Lachenbruch, B., McCulloh, KA, Johnson, DM, Woodruff, D.R.
879 Climate-related trends in sapwood biophysical properties in two conifers: avoidance of
880 hydraulic dysfunction through coordinated adjustments in xylem efficiency, safety and
881 capacitance. *Plant Cell Environ.* Apr;34(4):643-54. doi: 10.1111/j.1365-3040.2010.02269.x.
882 Epub 2011 Feb 11. PMID: 21309793. 2011
- 883 Bartlett, M.K., Klein, T., Jansen, S., Choat, B. and Sack, L., The correlations and sequence of
884 plant stomatal, hydraulic, and wilting responses to drought. *Proceedings of the National*
885 *Academy of Sciences*, 113(46), pp.13098-13103. 2016.
- 886 Brodribb, T.J., Bowman, D.J., Nichols, S., Delzon, S. and Burtlett, R., 2010. Xylem function and
887 growth rate interact to determine recovery rates after exposure to extreme water deficit.
888 *New Phytologist*, 188(2), pp.533-542.

- 889 Buotte, Polly C., Samuel Levis, Beverly E. Law, Tara W. Hudiburg, David E. Rupp, and Jeffery
890 J. Kent. “Near - Future Forest Vulnerability to Drought and Fire Varies across the Western
891 United States.” (July):1–14. 2018.
- 892 Canadell, J.G., Le Quéré, C., Raupach, M.R., Field, C.B., Buitenhuis, E.T., Ciais, P., Conway,
893 T.J., Gillett, N.P., Houghton, R.A. and Marland, G., Contributions to accelerating
894 atmospheric CO₂ growth from economic activity, carbon intensity, and efficiency of natural
895 sinks. *Proceedings of the national academy of sciences*, 104(47), pp.18866-18870. 2007.
- 896 Choat, Brendan, and Jarmila Pittermann. “New Insights into Bordered Pit Structure and
897 Cavitation Resistance in Angiosperms and Conifers.” *New Phytologist*: 555–57. 2009.
- 898 Christoffersen, B. O. et al. “Linking Hydraulic Traits to Tropical Forest Function in a Size-
899 Structured and Trait-Driven Model (TFS v . 1-Hydro).” : 4227–55. 2016.
- 900 Coley, P.D., Bryant, J.P. and Chapin, F.S., Resource availability and plant antiherbivore
901 defense. *Science*, 230(4728), pp.895-899. 1985.
- 902 Corcuera, L., Cochard, H., Gil-Pelegrin, E. and Notivol, E., Phenotypic plasticity in mesic
903 populations of *Pinus pinaster* improves resistance to xylem embolism (P 50) under severe
904 drought. *Trees*, 25(6), pp.1033-1042. 2011.
- 905 Craine, J.M., Tilman, D., Wedin, D., Reich, P., Tjoelker, M. and Knops, J., Functional traits,
906 productivity and effects on nitrogen cycling of 33 grassland species. *Functional*
907 *Ecology*, 16(5), pp.563-574. 2002.
- 908 Danabasoglu, G. et al. “The Community Earth System Model Version 2 (CESM2) Journal of
909 Advances in Modeling Earth Systems.” *Journal of Advances in Modeling Earth Systems* 2:
910 1–35. 2020.
- 911 Domec, J.C., Warren, J.M., Meinzer, F.C. *et al.* Native root xylem embolism and stomatal closure
912 in stands of Douglas-fir and ponderosa pine: mitigation by hydraulic
913 redistribution. *Oecologia* 141, 7–16 <https://doi.org/10.1007/s00442-004-1621-4>. 2004.
- 914 Fettig, Christopher J, Leif A Mortenson, M Bu, and Patra B Fou. “Tree Mortality Following
915 Drought in the Central and Southern Sierra Nevada, California, U.S.” *Forest Ecology and*
916 *Management* 432: 164–78. 2019.
- 917 Fisher, R. a. et al. “Taking off the Training Wheels: The Properties of a Dynamic Vegetation
918 Model without Climate Envelopes, CLM4.5(ED).” *Geoscientific Model Development* 8(11):
919 3593–3619. 2015.
- 920 Gaylord, M.L., Kolb, T.E. and McDowell, N.G.,. Mechanisms of piñon pine mortality after
921 severe drought: a retrospective study of mature trees. *Tree physiology*, 35(8), pp.806-816.
922 2015
- 923 Geen, Anthony Toby O et al. “Southern Sierra Critical Zone Observatory and Kings River
924 Experimental Watersheds : A Synthesis of Measurements , New Insights , and Future
925 Directions.” *Vadose Zone J. Advancing Critical Zone Science* *Advancing Critical Zone*
926 *Science*. 2018.
- 927 Gleason, Sean M., Mark Westoby, Steven Jansen, Brendan Choat, Uwe G. Hacke, Robert B.

- 928 Pratt, Radika Bhaskar, Tim J. Brodribb, Sandra J. Bucci, Kun Fang Cao, Hervé Cochard,
 929 Sylvain Delzon, Jean Christophe Domec, Ze Xin Fan, Taylor S. Feild, Anna L. Jacobsen,
 930 Daniel M. Johnson, Frederic Lens, Hafiz Maherali, Jordi Martínez-Vilalta, Stefan Mayr,
 931 Katherine A. Mcculloh, Maurizio Mencuccini, Patrick J. Mitchell, Hugh Morris, Andrea
 932 Nardini, Jarmila Pittermann, Lenka Plavcová, Stefan G. Schreiber, John S. Sperry, Ian J.
 933 Wright, and Amy E. Zanne. “Weak Tradeoff between Xylem Safety and Xylem-Specific
 934 Hydraulic Efficiency across the World’s Woody Plant Species.” *New Phytologist*
 935 209(1):123–36. 2016.
- 936 Golaz, Jean-Christophe, Luke P. Van Roekel, Xue Zheng, Andrew F. Roberts, Jonathan D.
 937 Wolfe, Wuyin Lin, Andrew M. Bradley et al. "The DOE E3SM Model Version 2: overview
 938 of the physical model and initial model evaluation." *Journal of Advances in Modeling Earth*
 939 *Systems* 14, no. 12 (2022).
- 940 Goulден, M L et al. “Evapotranspiration along an Elevation Gradient in California ’ s Sierra
 941 Nevada.” *Journal of Geophysical Research* 117(1): 1–13. 2015.
- 942 Goulден, M L, and R C Bales. 2019. “California Forest Die-off Linked to Multi-Year Deep Soil
 943 Drying in 2012–2015 Drought.” *Nature Geoscience* 12(August).
 944 <http://dx.doi.org/10.1038/s41561-019-0388-5>.
- 945 Grime, J.P., Evidence for the existence of three primary strategies in plants and its relevance to
 946 ecological and evolutionary theory. *The American Naturalist*, 111(982), pp.1169-1194.
 947 1977.
- 948 Grime, J.P., Plant strategies and vegetation processes. *Plant strategies and vegetation processes*.
 949 1979.
- 950 Hacke, Uwe G., Rachel Spicer, Stefan G. Schreiber, and Lenka Plavcová. “An Ecophysiological
 951 and Developmental Perspective on Variation in Vessel Diameter.” *Plant Cell and*
 952 *Environment* 40(6):831–45. 2017.
- 953 Hammond, W., K. Yu⁺, L. Wilson, R. Will, W.R.L. Anderegg, and H. Adams. 2019. “Dead or
 954 dying? Quantifying the point of no return from hydraulic failure in drought-induced tree
 955 mortality”. *New Phytologist*. doi: 10.1111/nph.15922. Published, 05/2019
- 956 Hartmann, Henrik, Waldemar Ziegler, Olaf Kolle, and Susan Trumbore. “Thirst Beats Hunger -
 957 Declining Hydration during Drought Prevents Carbon Starvation in Norway Spruce
 958 Saplings.” *New Phytologist* 200(2):340–49. 2013.
- 959 Hartung, Wolfram, Angela Sauter, and Eleonore Hose. “Abscisic Acid in the Xylem : Where
 960 Does It Come from , Where Does It Go To ?” 53(366): 27–32. 2002.
- 961 Hetherington, Alistair M, and F Ian Woodward. “The Role of Stomata in Sensing and Driving
 962 Environmental Change.” *Nature* 424(August): 901–8. 2003.
- 963 Huang, J., Kautz, M., Trowbridge, A. M., Hammerbacher, A., Raffa, K. F., Adams, H. D., ... &
 964 Gershenson, J. Tree defence and bark beetles in a drying world: carbon partitioning,
 965 functioning and modelling. *New Phytologist*, 225(1), 26-36. (2020).
- 966 Inouea, Shin-ichiro, and Toshinori Kinoshitaa. 2017. “Blue Light Regulation of Stomatal
 967 Opening and the Plasma Membrane H⁺-ATPase 2.” *Plant Physiology* (166): 17.

- 968 Ivanov, Valeriy Y., Lucy R. Hutyrá, Steven C. Wofsy, J. William Munger, Scott R. Saleska,
969 Raimundo C. De Oliveira, and Plínio B. De Camargo. “Root Niche Separation Can Explain
970 Avoidance of Seasonal Drought Stress and Vulnerability of Overstory Trees to Extended
971 Drought in a Mature Amazonian Forest.” *Water Resources Research* 48(12):1–21. 2012.
- 972 Jackson, R.B., Canadell, J., Ehleringer, J.R., Mooney, H.A., Sala, O.E. and Schulze, E.D., A
973 global analysis of root distributions for terrestrial biomes. *Oecologia*, 108(3), pp.389-411.
974 1996.
- 975 Johnson, D. M., Domec, J. C., Carter Berry, Z., Schwantes, A. M., McCulloh, K. A., Woodruff,
976 D. R., ... & McDowell, N. G. Co-occurring woody species have diverse hydraulic strategies
977 and mortality rates during an extreme drought. *Plant, Cell & Environment*, 41(3), 576-588.
978 2018.
- 979 Kattge, J., Bönišch, G., Díaz, S., Lavorel, S., Prentice, I. C., Leadley, P., Tautenhahn, S., Werner,
980 G., et al. “TRY Plant Trait Database - Enhanced Coverage and Open Access.” *Global
981 Change Biology* 26(1):119–88. 2020.
- 982 Kelly, Anne E, and Michael L Goulden. “A Montane Mediterranean Climate Supports Year-
983 Round Photosynthesis and High Forest Biomass.” : 459–68. 2016.
- 984 Khasanova, Albina, John T. Lovell, Jason Bonnette, Xiaoyu Weng, Jerry Jenkins, Yuko
985 Yoshinaga, Jeremy Schmutz, and Thomas E. Juenger. “The Genetic Architecture of Shoot
986 and Root Trait Divergence between Mesic and Xeric Ecotypes of a Perennial Grass.”
987 *Frontiers in Plant Science* 10(April):1–10. 2019.
- 988 Kilgore, J.S., Jacobsen, A.L. and Telewski, F.W., Hydraulics of Pinus (subsection Ponderosae)
989 populations across an elevation gradient in the Santa Catalina Mountains of southern
990 Arizona. *Madroño*, 67(4), pp.218-226. 2021.
- 991 Klos, P Zion et al. “Subsurface Plant-Accessible Water in Mountain Ecosystems with a
992 Mediterranean Climate.” *Wiley Interdisciplinary Reviews: Water* (May 2017): 1–14. 2017.
- 993 Koch, G.W. and Fredeen, A.L., Transport challenges in tall trees. In *Vascular transport in
994 plants* (pp. 437-456). Academic Press. 2005.
- 995 Koven, C.D., Knox, R.G., Fisher, R.A., Chambers, J.Q., Christoffersen, B.O., Davies, S.J.,
996 Detto, M., Dietze, M.C., Faybishenko, B., Holm, J. and Huang, M., Benchmarking and
997 parameter sensitivity of physiological and vegetation dynamics using the Functionally
998 Assembled Terrestrial Ecosystem Simulator (FATES) at Barro Colorado Island,
999 Panama. *Biogeosciences*, 17(11), pp.3017-3044. 2020.
- 1000 Kulmatiski, Andrew and Karen H. Beard. “Root Niche Partitioning among Grasses, Saplings,
1001 and Trees Measured Using a Tracer Technique.” *Oecologia* 171(1):25–37. 2013.
- 1002 Lawrence, D.M., Fisher, R.A., Koven, C.D., Oleson, K.W., Swenson, S.C., Bonan, G., Collier,
1003 N., Ghimire, B., van Kampenhout, L., Kennedy, D. and Kluzek, E., The Community Land
1004 Model version 5: Description of new features, benchmarking, and impact of forcing
1005 uncertainty. *Journal of Advances in Modeling Earth Systems*, 11(12), pp.4245-4287.
- 1006 Li, S., Lens, F., Espino, S., Karimi, Z., Klepsch, M., Schenk, H.J., Schmitt, M., Schuldt, B. and

- 1007 Jansen, S., 2016. Intervessel pit membrane thickness as a key determinant of embolism
1008 resistance in angiosperm xylem. *Iawa Journal*, 37(2), pp.152-171. 2019.
- 1009 Lu, Yaojie et al. 2019. “Optimal Stomatal Drought Response Shaped by Competition for Water
1010 and Hydraulic Risk Can Explain Plant Trait Covariation.” (1977).
- 1011 Mackay, D. S., Savoy, P. R., Grossiord, C., Tai, X., Pleban, J. R., Wang, D. R., ... & Sperry, J. S.
1012 Conifers depend on established roots during drought: results from a coupled model of
1013 carbon allocation and hydraulics. *New Phytologist*, 225(2), 679-692. 2020.
- 1014 Martínez-Vilalta, Jordi, Anna Sala, and Josep Piñol. *The Hydraulic Architecture of Pinaceae-a*
1015 *Review*. Vol. 171. 2004.
- 1016 Matheny, Ashley M, Golnazalsadat Mirfenderesgi, and Gil Bohrer. “Trait-Based Representation
1017 of Hydrological Functional Properties of Plants in Weather and Ecosystem Models.” *Plant*
1018 *Diversity* 39(1): 1–12. <http://dx.doi.org/10.1016/j.pld.2016.10.001>. 2017.
- 1019 Matheny, A.M., Fiorella, R.P., Bohrer, G., Poulsen, C.J., Morin, T.H., Wunderlich, A., Vogel,
1020 C.S. and Curtis, P.S., Contrasting strategies of hydraulic control in two codominant
1021 temperate tree species. *Ecology*, 10(3), p.e1815. 2017.
- 1022 McDowell, Nate, Nate McDowell, William T. Pockman, Craig D. Allen, D. David, Neil Cobb,
1023 Thomas Kolb, Jennifer Plaut, John Sperry, Adam West, David G. Williams, and Enrico A.
1024 Yezzer. “Mechanisms of Plant Survival and Mortality during Drought : Why Do Some
1025 Plants Survive While Others Succumb To.” 2008.
- 1026 McDowell, Nate G. et al. “Evaluating Theories of Drought-Induced Vegetation Mortality Using
1027 a Multimodel – Experiment Framework.” : 304–21. 2013.
- 1028 Mooney, Harold and Erika Zavaleta. *Ecosystems of California*. Vol. 3. edited by H. Mooney and
1029 E. Zavaleta. Oakland, California, USA: Univ of California Press. 2003.
- 1030 Mursinna, A. Rio, Erica McCormick, Kati Van Horn, Lisa Sartin, and Ashley M. Matheny.
1031 “Plant Hydraulic Trait Covariation: A Global Meta-Analysis to Reduce Degrees of Freedom
1032 in Trait-Based Hydrologic Models.” *Forests* 9(8). 2018.
- 1033 Oleson, Keith W et al. “Technical Description of Version 4.5 of the Community Land Model
1034 (CLM) Coordinating.” In *Natl. Cent. Atmos. Res. Tech. Note*, Natl. Cent. for Atmos. Res.,
1035 Boulder, Colo. 2013.
- 1036 Pittermann, Jarmila, John S. Sperry, Uwe G. Hacke, James K. Wheeler, and Elzard H. Sikkema.
1037 “Inter-Tracheid Pitting and the Hydraulic Efficiency of Conifer Wood: The Role of
1038 Tracheid Allometry and Cavitation Protection.” *American Journal of Botany* 93(9):1265–
1039 73. 2006.
- 1040 Pittermann, Jarmila, John S. Sperry, James K. Wheeler, Uwe G. Hacke, and Elzard H. Sikkema.
1041 “Mechanical Reinforcement of Tracheids Compromises the Hydraulic Efficiency of Conifer
1042 Xylem.” *Plant, Cell and Environment* 29(8):1618–28. 2006.
- 1043 Pockman, W.T. and Sperry, J.S., Vulnerability to xylem cavitation and the distribution of
1044 Sonoran desert vegetation. *American journal of botany*, 87(9), pp.1287-1299. 2000.

- 1045 Powell, Thomas L., James K. Wheeler, Alex A. R. de Oliveira, Antonio Carlos Lola da Costa,
1046 Scott R. Saleska, Patrick Meir, and Paul R. Moorcroft. "Differences in Xylem and Leaf
1047 Hydraulic Traits Explain Differences in Drought Tolerance among Mature Amazon
1048 Rainforest Trees." *Global Change Biology* 23(10):4280–93. 2017.
- 1049 Pratt, R.B. and Jacobsen, A.L., Conflicting demands on angiosperm xylem: tradeoffs among
1050 storage, transport and biomechanics. *Plant, Cell & Environment*, 40(6), pp.897-913. 2017.
- 1051 Reich, Peter B., Ian J. Wright, Jeannine Cavender-Bares, J. M. Craine, Jacek Oleksyn, M.
1052 Westoby, and M. B. Walters. "The evolution of plant functional variation: traits, spectra,
1053 and strategies." *International Journal of Plant Sciences* 164, no. S3: S143-S164. (2003).
- 1054 Reichstein, M., Bahn, M., Mahecha, M.D., Kattge, J. and Baldocchi, D.D., Linking plant and
1055 ecosystem functional biogeography. *Proceedings of the National Academy of
1056 Sciences*, 111(38), pp.13697-13702. 2014.
- 1057 Rodriguez-Dominguez, C.M., Buckley, T.N., Egea, G., de Cires, A., Hernandez-Santana, V.,
1058 Martorell, S. and Diaz-Espejo, A., Most stomatal closure in woody species under moderate
1059 drought can be explained by stomatal responses to leaf turgor. *Plant, Cell &
1060 Environment*, 39(9), pp.2014-2026. 2016.
- 1061 Rowland, L., A. C. L. Da Costa, D. R. Galbraith, R. S. Oliveira, O. J. Binks, A. A. R. Oliveira,
1062 A. M. Pullen, C. E. Doughty, D. B. Metcalfe, S. S. Vasconcelos, L. V. Ferreira, Y. Malhi, J.
1063 Grace, M. Mencuccini, and P. Meir. "Death from Drought in Tropical Forests Is Triggered
1064 by Hydraulics Not Carbon Starvation." *Nature* 528(7580):119–22. 2015.
- 1065 Salmon, Yann, José M. Torres-Ruiz, Rafael Poyatos, Jordi Martinez-Vilalta, Patrick Meir, Hervé
1066 Cochard, and Maurizio Mencuccini. "Balancing the Risks of Hydraulic Failure and Carbon
1067 Starvation: A Twig Scale Analysis in Declining Scots Pine." *Plant Cell and Environment*
1068 38(12):2575–88. 2015.
- 1069 Sauter, Angela, W J Davies, Wolfram Hartung, and Lehrstuhl Botanik I. "The Long-Distance
1070 Abscisic Acid Signal in the Droughted Plant : The Fate of the Hormone on Its Way from
1071 Root to Shoot." 52(363): 1991–97. 2001.
- 1072 Skelton, R. P., West, A. G., & Dawson, T. E. "Predicting plant vulnerability to drought in
1073 biodiverse regions using functional traits." *Proceedings of the National Academy of
1074 Sciences*, 112(18), 5744-5749. 2015.
- 1075 Sevanto, Sanna, Nate G. McDowell, L. Turin Dickman, Robert Pangle, and William T. Pockman.
1076 "How Do Trees Die? A Test of the Hydraulic Failure and Carbon Starvation Hypotheses."
1077 *Plant, Cell and Environment* 37(1):153–61. 2014.
- 1078 Sperry, John S. "Evolution of Water Transport and Xylem Structure." *International Journal of
1079 Plant Sciences* 164. 2003.
- 1080 Teuling, Adriaan J, Remko Uijlenhoet, and Peter A Troch. "Impact of Plant Water Uptake
1081 Strategy on Soil Moisture and Evapotranspiration Dynamics during Drydown." 33: 3–7.
1082 2006.
- 1083 Vesala, T., Sevanto, S., Grönholm, T., Salmon, Y., Nikinmaa, E., Hari, P. and Hölttä, T., Effect

- 1084 of leaf water potential on internal humidity and CO₂ dissolution: reverse transpiration and
1085 improved water use efficiency under negative pressure. *Frontiers in plant science*, 8, p.54.
1086 2017.
- 1087 Westoby, M., Falster, D.S., Moles, A.T., Vesk, P.A. and Wright, I.J., Plant ecological strategies:
1088 some leading dimensions of variation between species. *Annual review of ecology and*
1089 *systematics*, 33(1), pp.125-159. 2002.
- 1090 Wilkinson, S, and W J Davies. “ABA-Based Chemical Signalling : The Co-Ordination Of.” :
1091 195–210. 2002.
- 1092 Wullschleger, Stan D. et al. “Plant Functional Types in Earth System Models : Past Experiences
1093 and Future Directions for Application of Dynamic Vegetation Models in High-Latitude
1094 Ecosystems.” *Annals of botany* (114): 1–16. 2014.
- 1095 Yu, Gui-rui, Jie Zhuang, and Keiichi Nakayamma. “Root Water Uptake and Profile Soil Water
1096 as Affected by Vertical Root Distribution.” *Plant Ecol*: 15–30. 2007.
- 1097 Zeng, Xubin. “Global Vegetation Root Distribution for Land Modeling.” *Journal of*
1098 *Hydrometeorology* 2(5): 525–30. 2001.
- 1099
- 1100

1101 **Tables**

1102 **Table 1 Parameters used in FATES-Hydro sensitivity analysis**

1103

Parameters	Biological meaning	Values	Units
r_a, r_b	Root distribution: shallow roots vs. deep roots	(0.1, 0.1) – (2 5)	unitless
$P50_{gs}$	Leaf xylem water potential at half stomatal closure stomatal control on safety vs. efficiency	$P50_x - P20_x$	Mpa
$P50_x$	Xylem water potential when xylem loss half of the conductance	-3.0 ^a , -4.8 ^b	Mpa
K_{max}	Maximum xylem conductivity per unit sap area	0.88 ^a , 0.64 ^b	kg/MPa/m/s
A	Shape parameter of van Genuchten hydrologic function	0.11855 ^a , 0.088026 ^b	Mpa ⁻¹
m, n	Shape parameters of van Genuchten hydrologic function	(0.8, 1.25) ^a , (0.8, 1.5) ^b	unitless

1104 a: values for efficient/unsafe xylem

1105 b: values for inefficient/safe xylem

1106

1107 **Table 2. List of major parameters**

1108

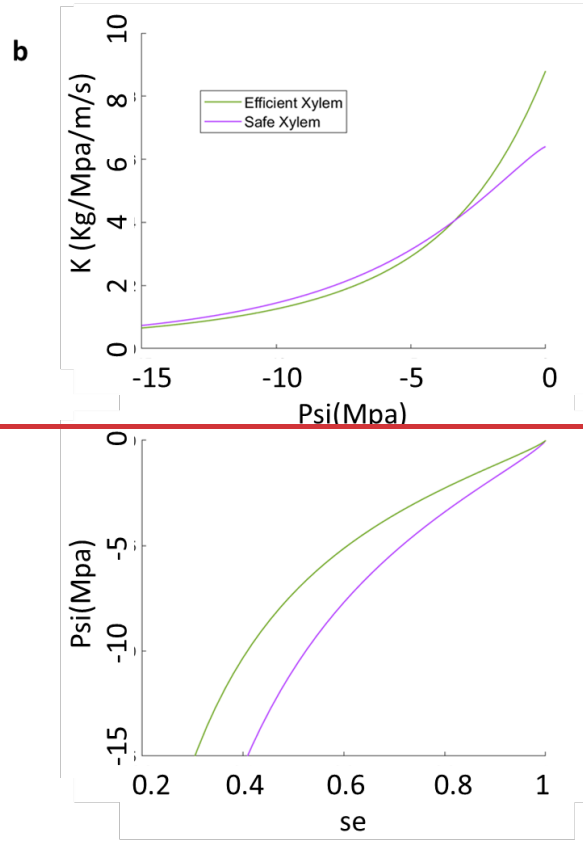
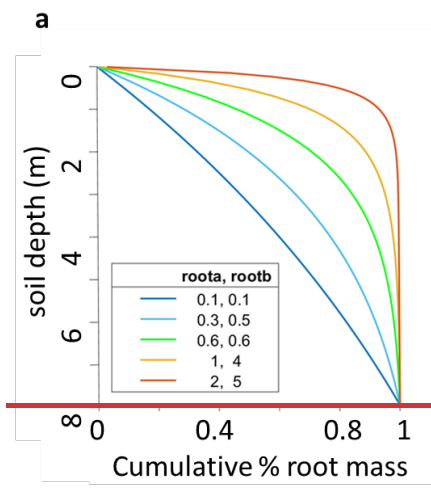
Symbol	Source code name	Value	Units	Description	Source
a_{gs}	fates_hydr_avuln_gs	2.5	unitless	shape parameter for stomatal control of water vapor (slope) exiting leaf	Christoffersen et al., 2016
χ	fates_hydr_p_taper	0.333	unitless	xylem taper exponent	Christoffersen et al., 2016
$\pi_{o,l}, \pi_{o,s}, \pi_{o,r}$	fates_hydr_pinot_node	-1.47, -1.23, -1.04	MPa	osmotic potential at full turgor of leaf, stem, root	Christoffersen et al., 2016
$RWC_{res,l}, RWC_{res,s}, RWC_{res,r}$	fates_hydr_resid_node	0.25, 0.325, 0.15	proportion	residual fraction of leaf, stem, root	Christoffersen et al., 2016
$\Theta_{sat,x}$	fates_hydr_thetas_node	0.65	cm ³ /cm ³	saturated water content of xylem	Christoffersen et al., 2016
SLA_{max}	fates_leaf_slamax	0.01	m ² /gC	Maximum Specific Leaf Area (SLA)	TRY
SLA_{top}	fates_leaf_slatop	0.01	m ² /gC	Specific Leaf Area (SLA) at top of canopy, projected area basis	TRY
$V_{cmax,25, top}$	fates_leaf_vcmax25top	55	umol CO ₂ /m ² /s	maximum carboxylation rate of Rub. at 25C, canopy top	TRY
$\frac{b_{opt}}{b_{opt}}$	fates_bbopt_c3	10000	umol H ₂ O/m ² /s	Ball-Berry minimum leaf stomatal conductance for C3 plants	Calibrated

1109

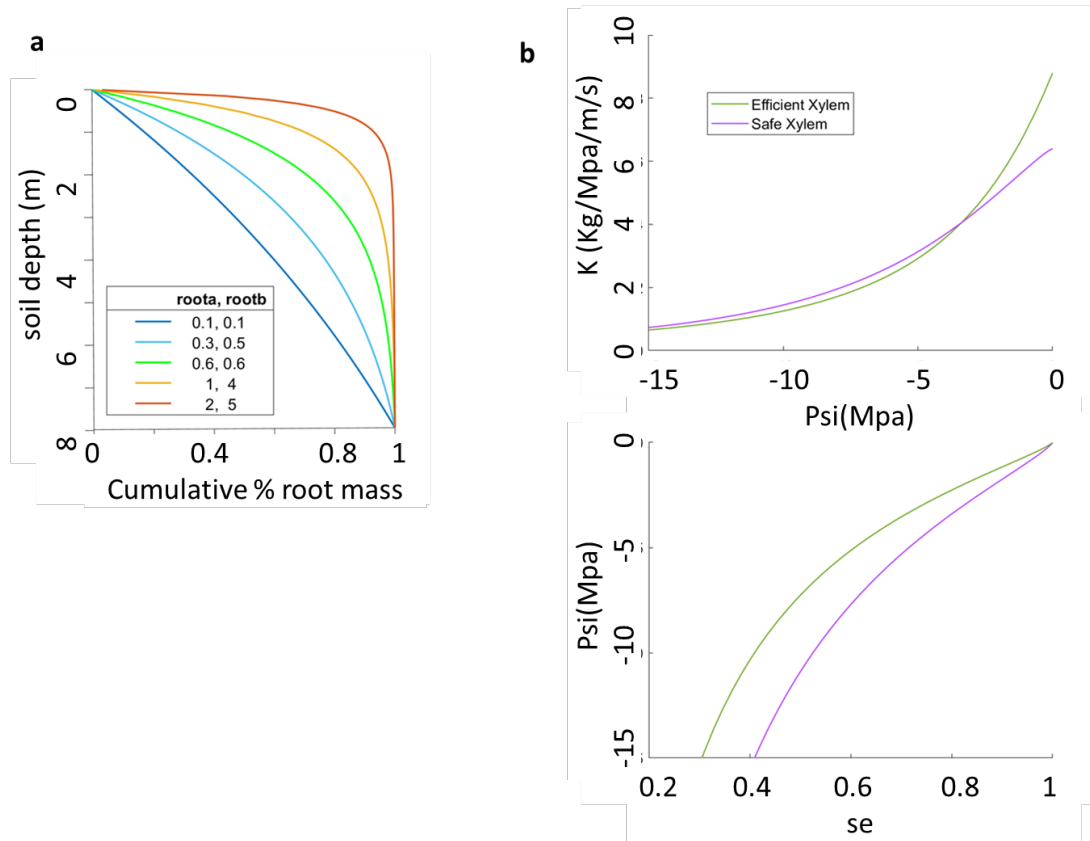
1110

1111 **Figures**

1112 Figure 1



1113



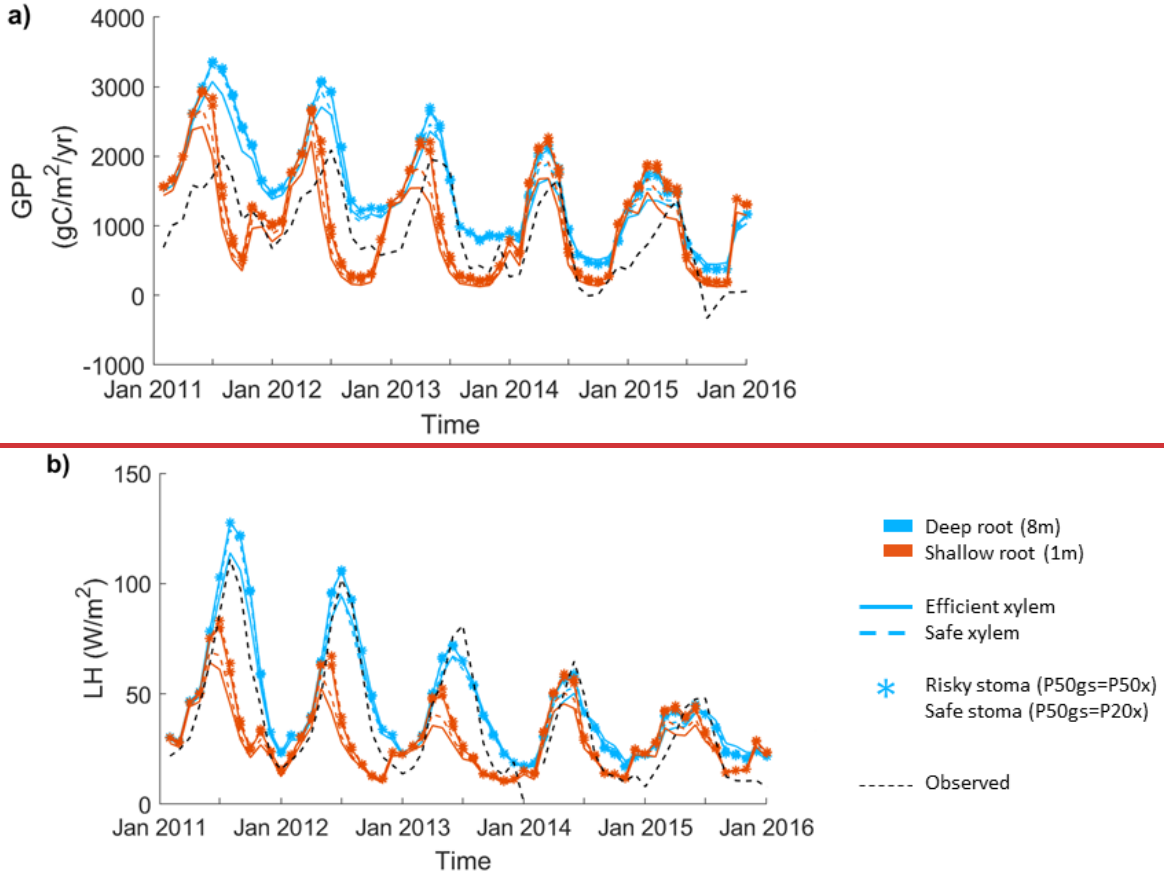
1114

1115

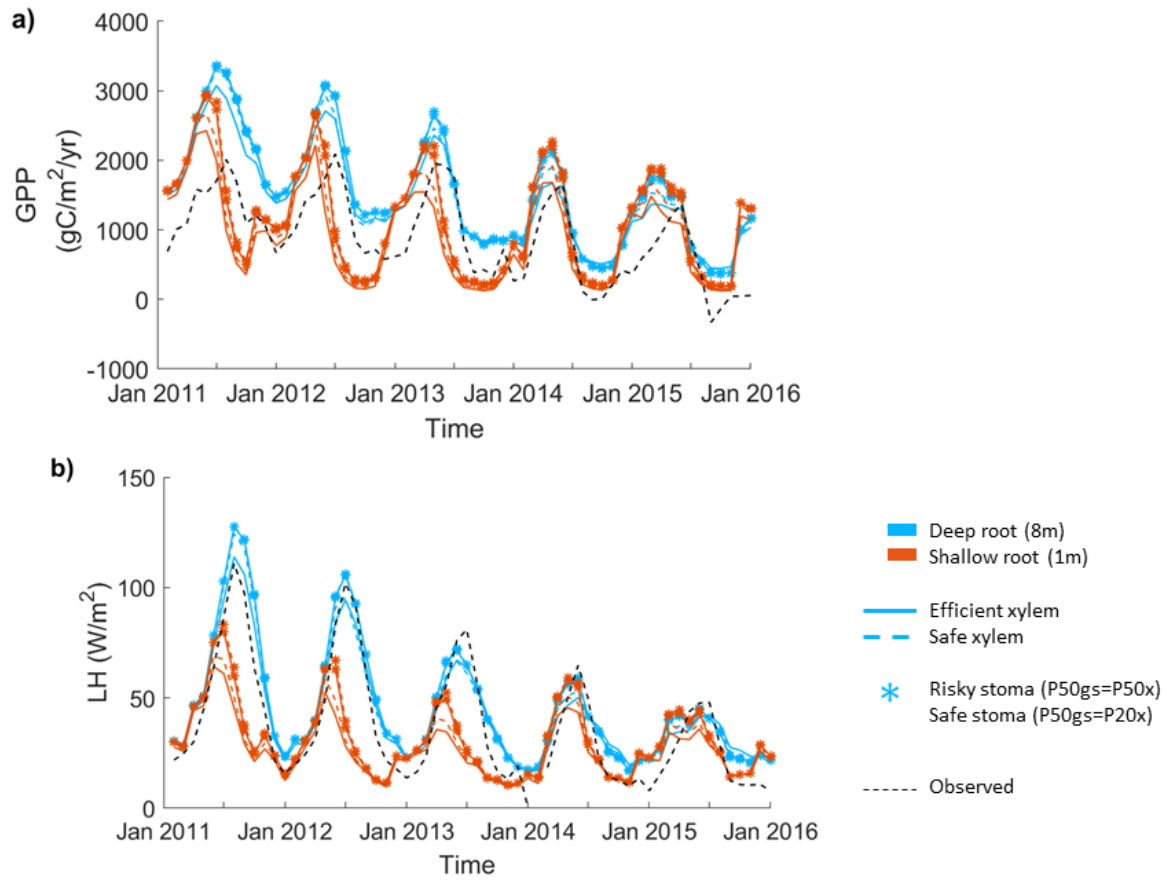
1116 Figure 1. Sensitivity analysis set up for: a) root parameters that give five root distribution
 1117 scenarios with effective rooting depths of 1m, 3m, 5m, 6.5m, and 8m , and b) two xylem
 1118 scenarios for safe xylem ($P_{50x}=-4.8$, $K_{max}=0.64$), and efficient xylem ($P_{50x}=-2.5$,
 1119 $K_{max}=0.88$).

1120

1121 Figure 2



1122

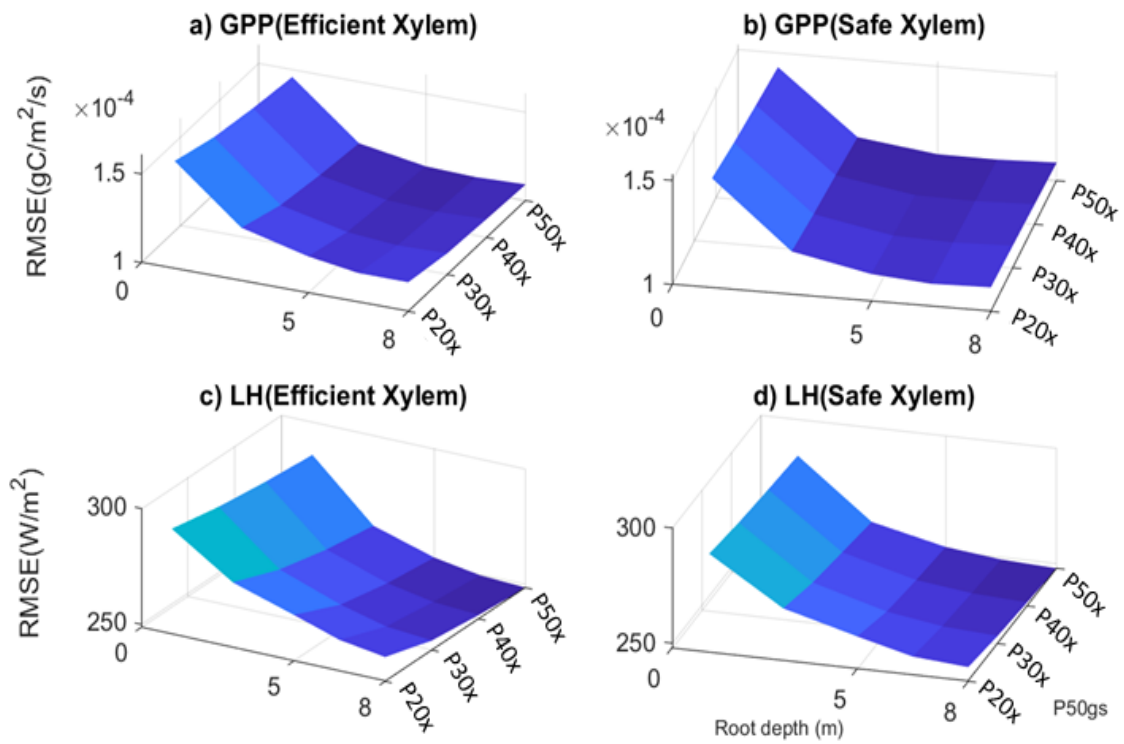
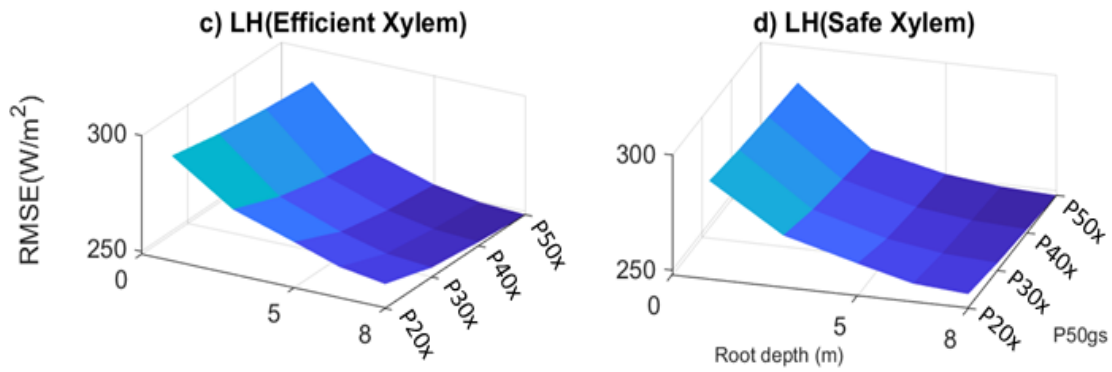
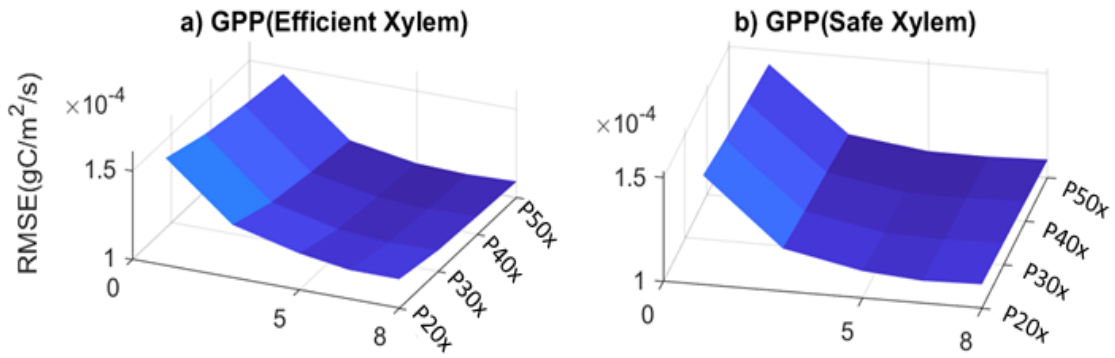


1123

1124 Figure 2. Impact of hydraulic strategies on ecosystem water and energy fluxes: a) monthly mean
 1125 gross primary productivity, and B) monthly mean latent heat flux, of the end member cases.

1126

1127



1129

1130

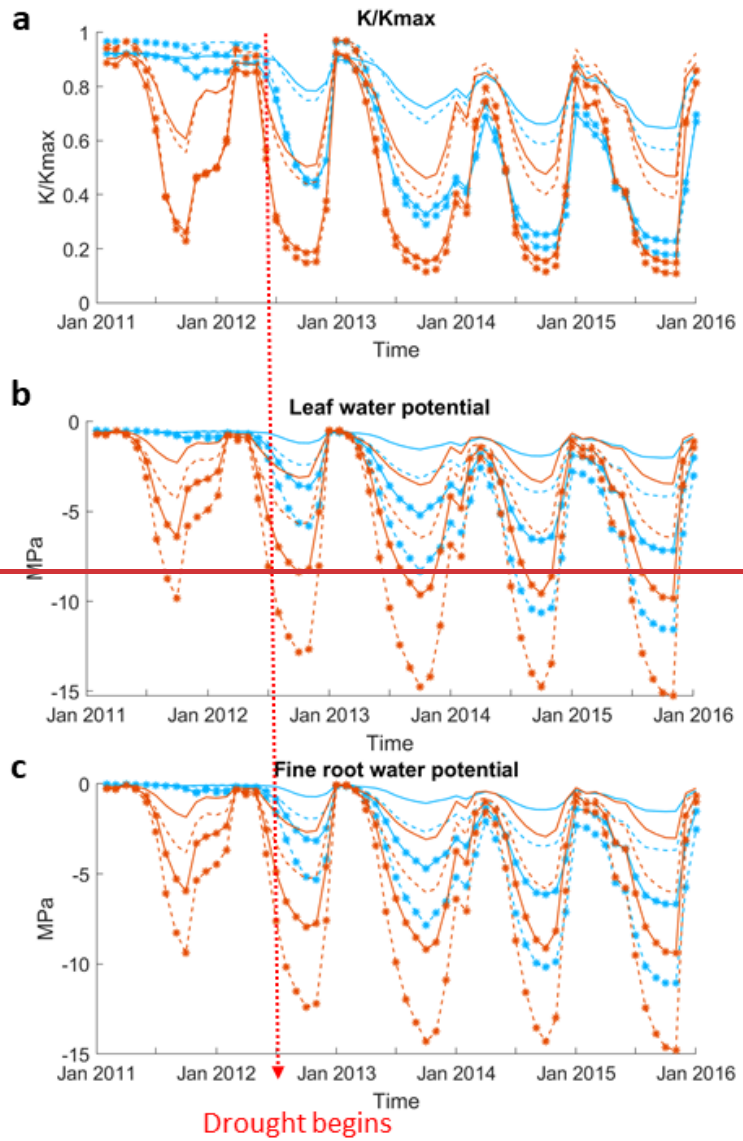
1131 Figure 3. Root mean square error of GPP (a-b), and latent heat flux (c-d) with respect to variation
1132 in input parameters.

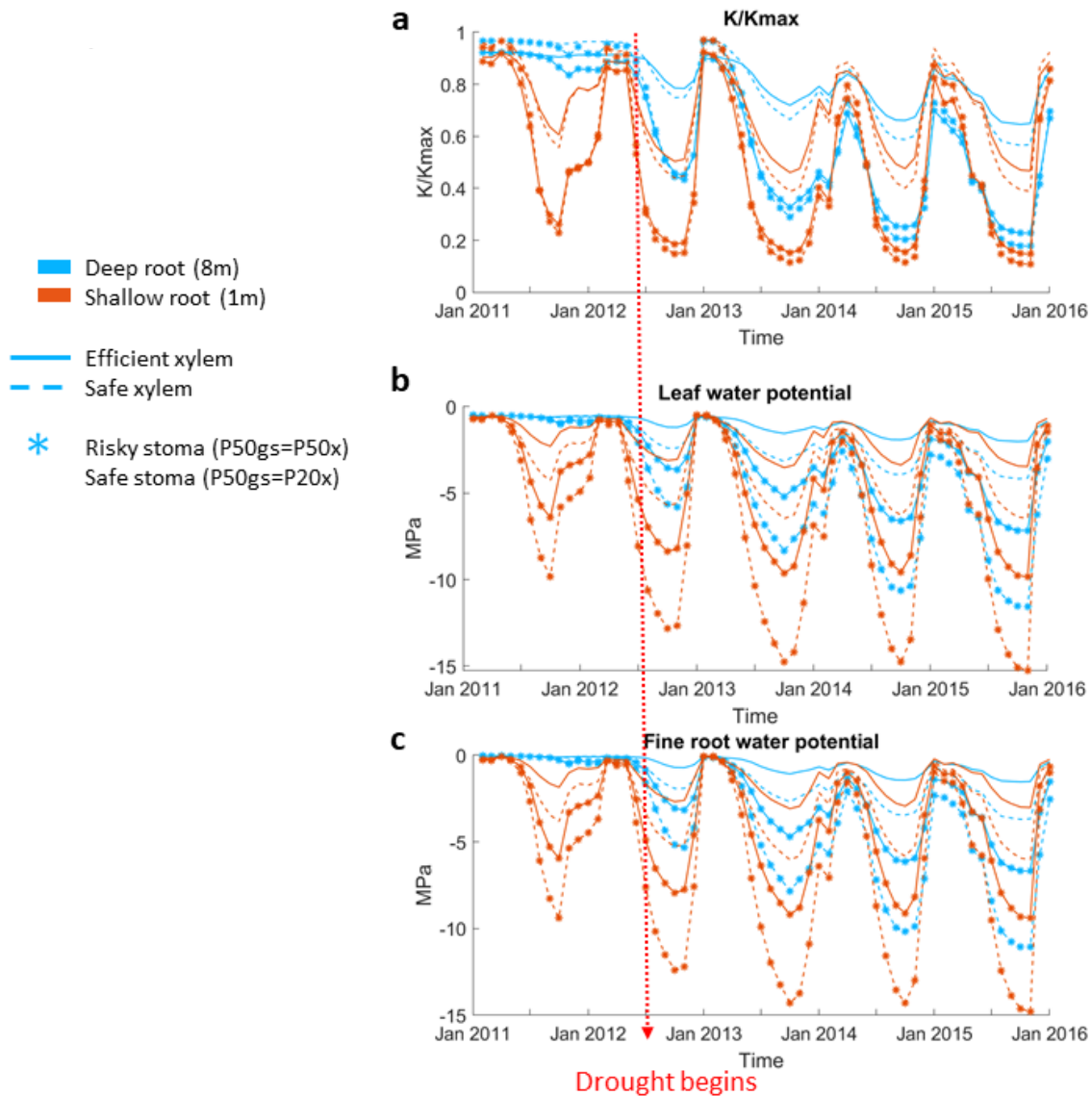
1133

1134

fig4

- Deep root (8m)
- Shallow root (1m)
- Efficient xylem
- Safe xylem
- * Risky stoma ($P_{50gs}=P_{50x}$)
- Safe stoma ($P_{50gs}=P_{20x}$)



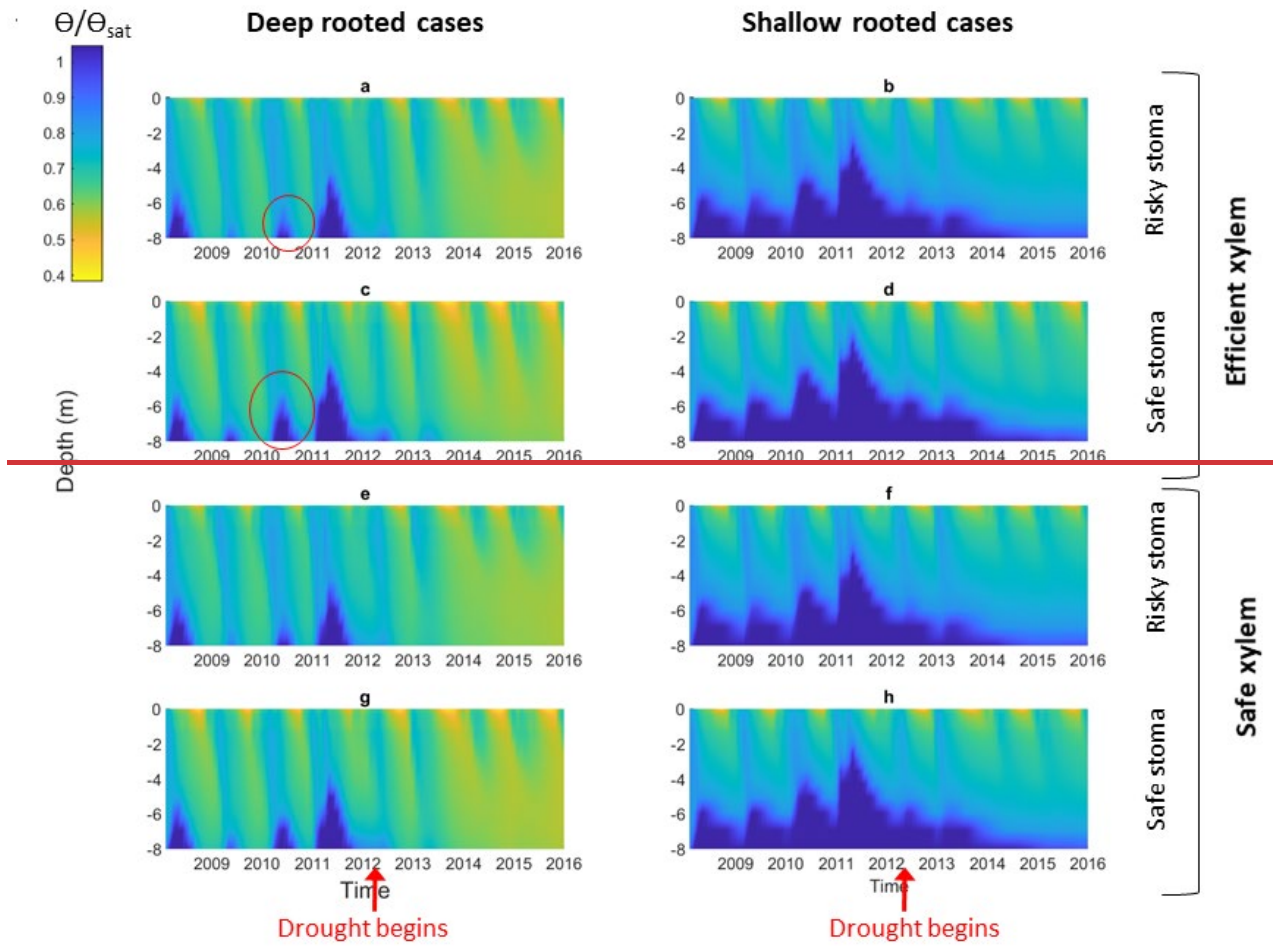


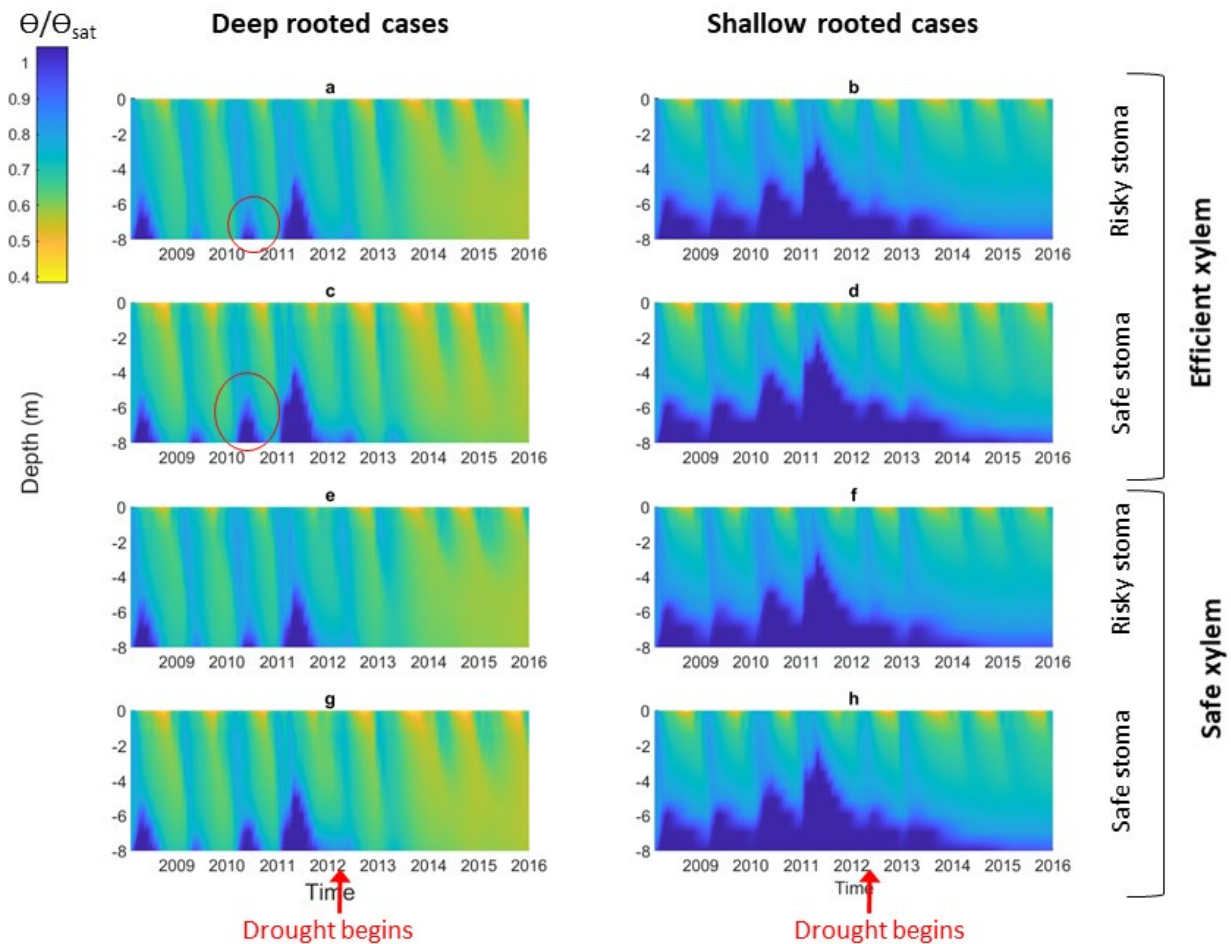
1138

1139 Figure 4. Seasonal and inter-annual variation of plant physiologic characteristics: a) monthly
 1140 mean stem fraction of conductance K/K_{\max} (a), monthly mean leaf water potential, and c)
 1141 monthly mean overall absorbing roots water potential, of the 55cm DBH cohort throughout the
 1142 2011-2015 period.

1143

1144





1147

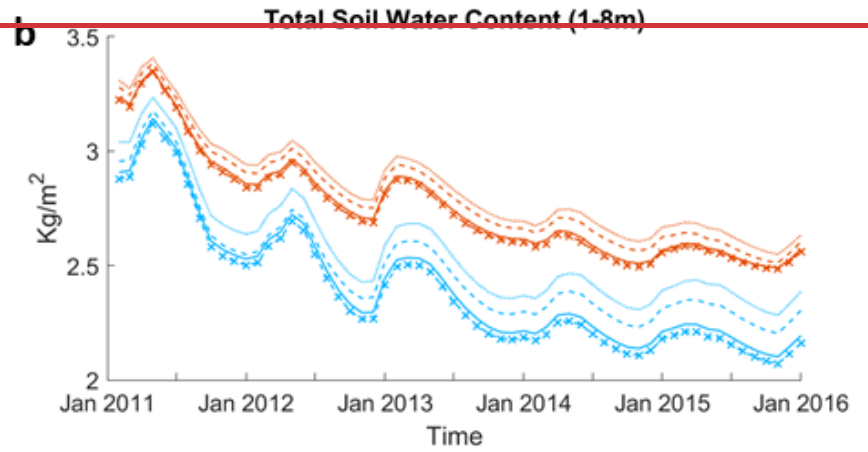
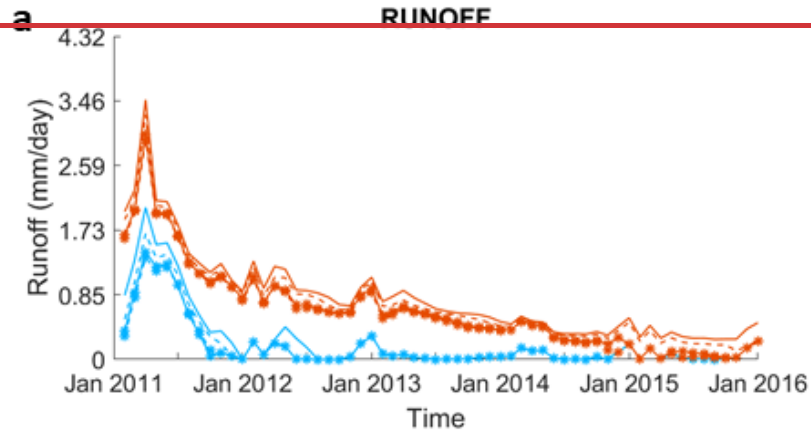
1148 Figure 5. Impact of different combination of rooting depth, xylem and stomatal traits on soil
 1149 moisture; left column shows deep rooted cases with a) efficient xylem and risky stoma, c)
 1150 efficient xylem and safe stoma, e) safe xylem and risky stoma, g) safe xylem and safe stoma.
 1151 Right column shows shallow rooted cases with b) efficient xylem and risky stoma, d) efficient
 1152 xylem and safe stoma, f) safe xylem and risky stoma, h) safe xylem and safe stoma; red cycle
 1153 highlights the effect of stomatal traits on deep water storage during the wet season of the pre-
 1154 drought period

1155

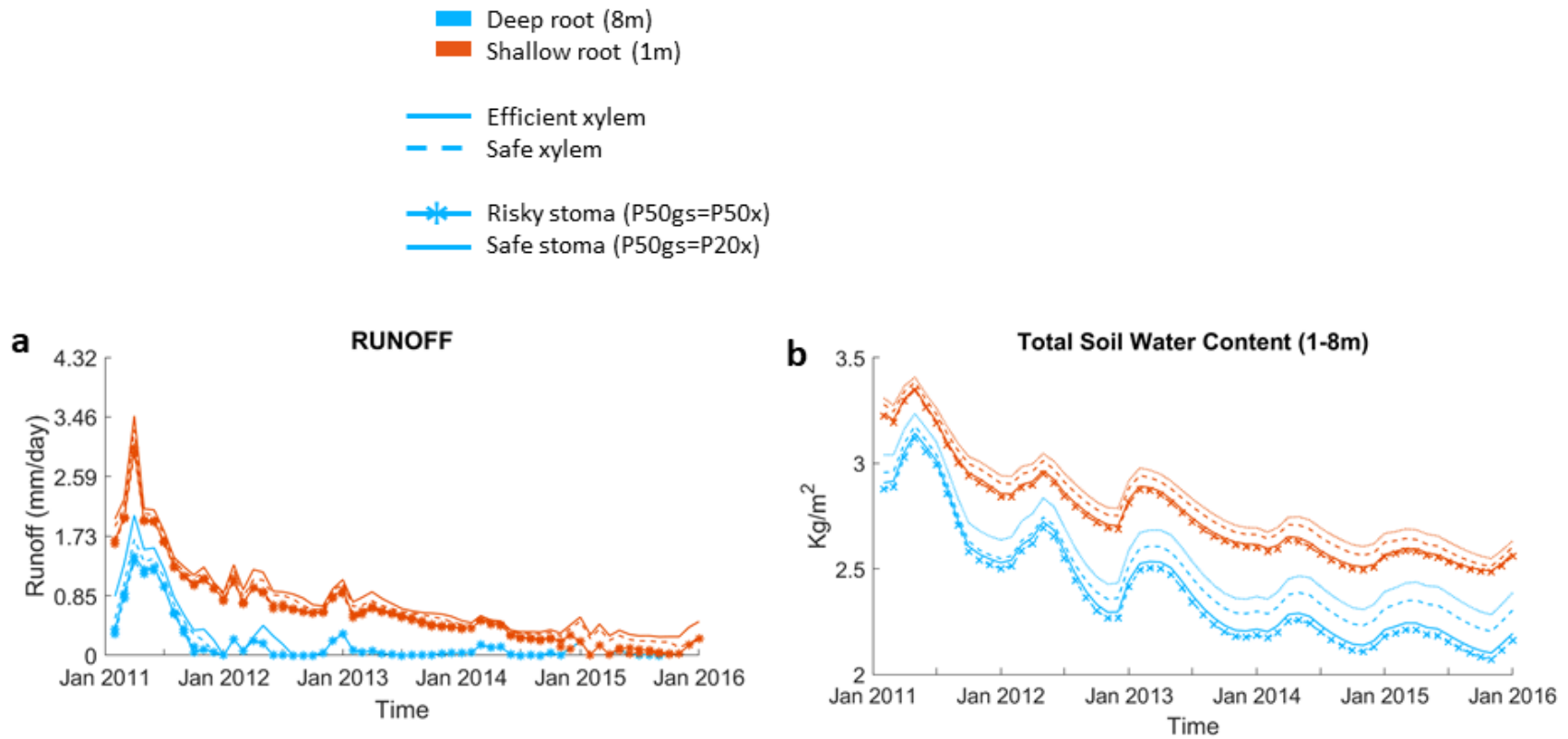
1156

1157 Figure 6
1158

- Deep root (8m)
- Shallow root (1m)
- Efficient xylem
- - Safe xylem
- *— Risky stoma (P50gs=P50x)
- Safe stoma (P50gs=P20x)

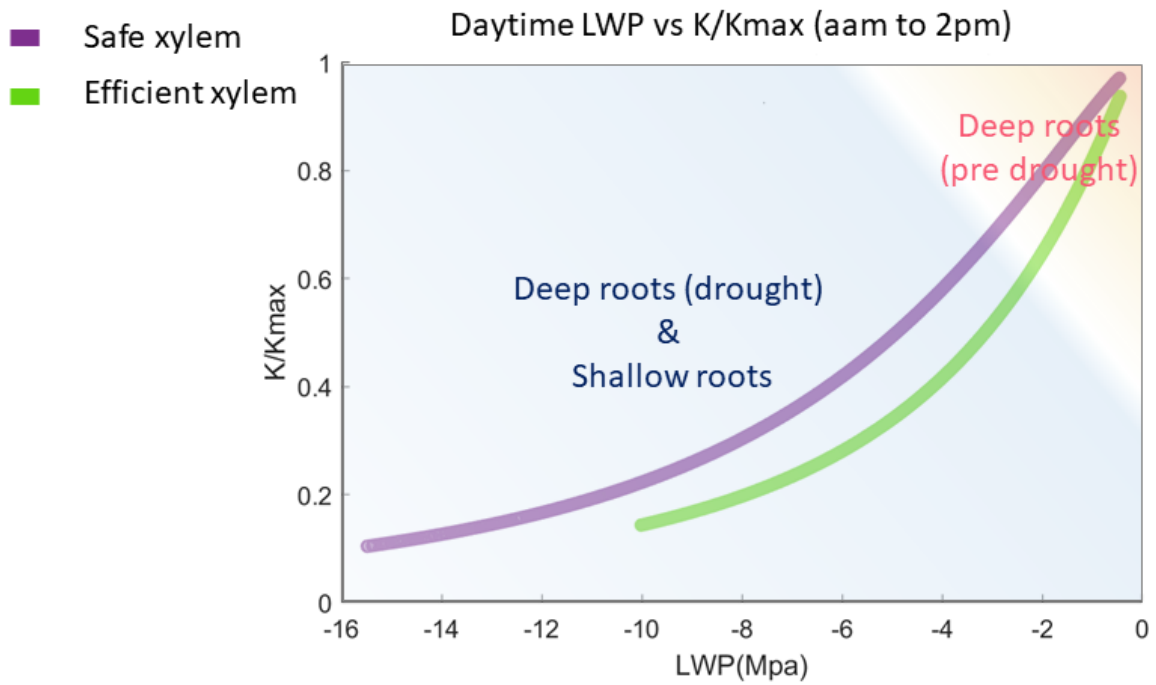
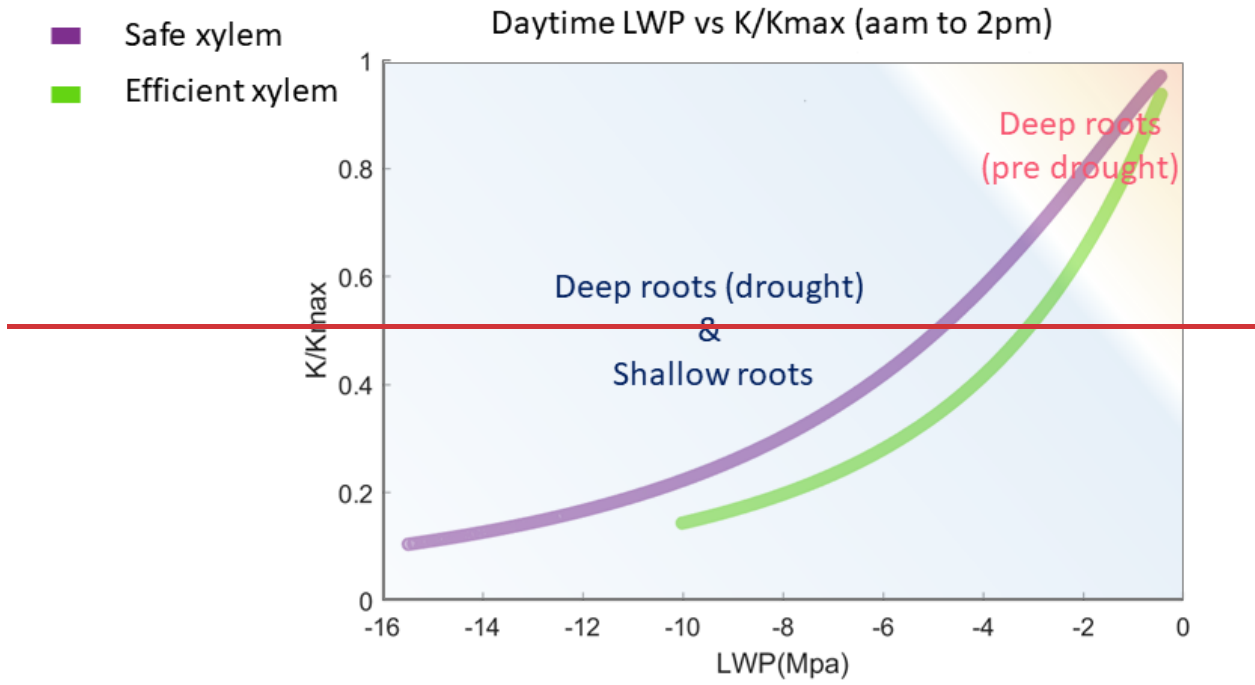


1159
1160



1161

1162 Figure 6. Impact on hydrologic processes: a) mean monthly total runoff, and b) monthly mean total soil water content of the entire soil
 1163 column.

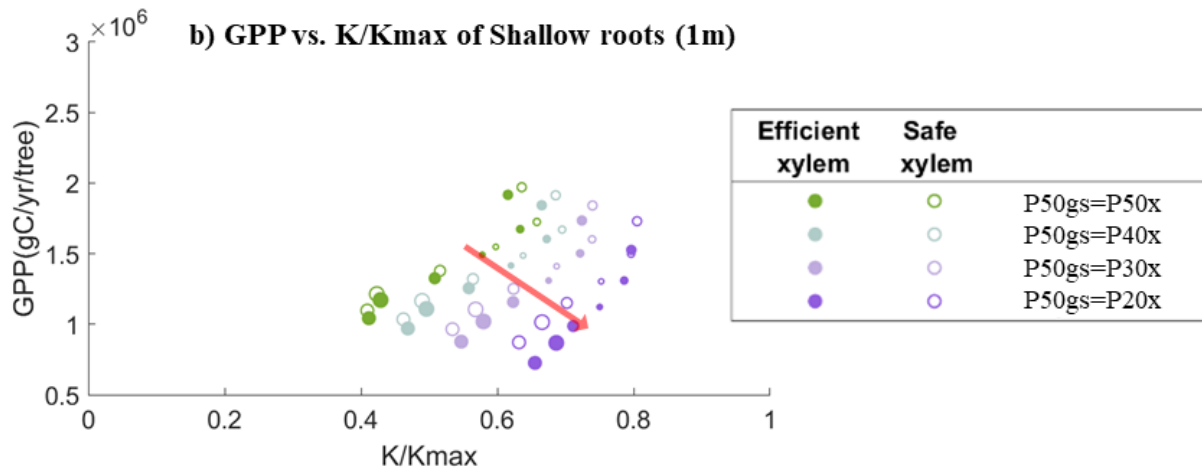
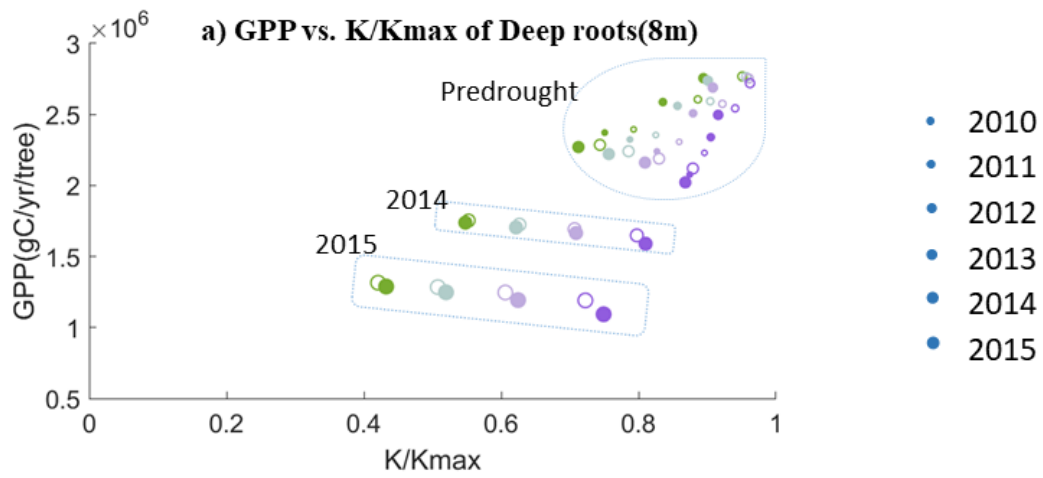


1167 Figure 7. Simulated leaf water potential and fraction loss of conductivity (K/K_{max}) of all the
1168 cases, which follow the two vulnerability curves.

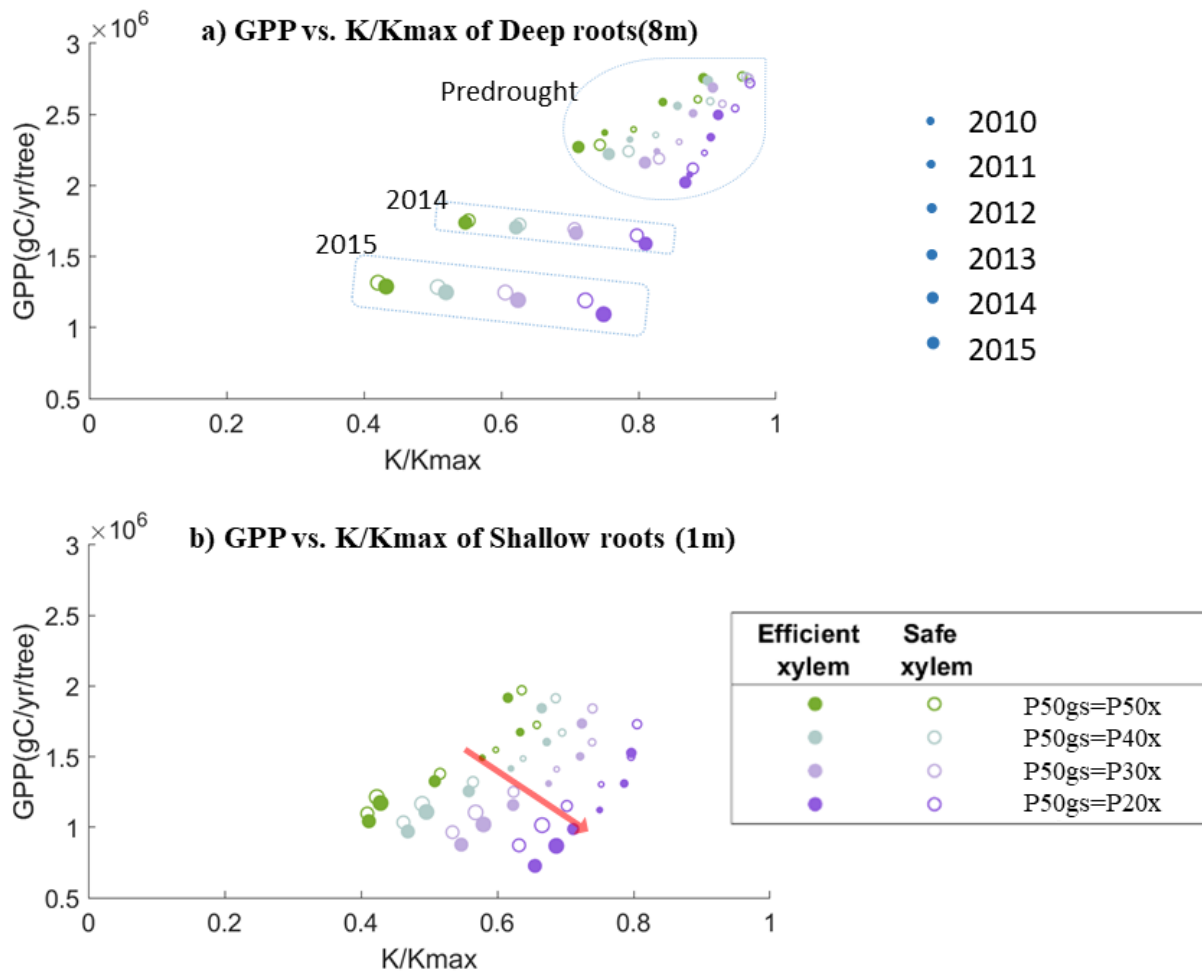
1169

1170

1171 Figure 8



1172



1173

1174 Figure 8. Simulated average annual GPP and fraction of conductance of a 55cm DBH cohort
 1175 with a) deep roots (effective rooting depth= 8m) and b) shallow roots (effective rooting depth=
 1176 1m).

1177